SPACE SCIENCES LABORATORY

[redacted]

UNIVERSITY OF CALIFORNIA

BERKELEY, CALIFORNIA

SPACE SCIENCES LABORATORY
University of California
Berkeley, California

GENERATION OF FLOW FIELDS IN PARTICLE FUELED COMBUSTION SYSTEMS

by

C. W. BUSCH

A. J. LADERMAN
Project Director

A. K. OPPENHEIM
Faculty Investigator

Technical Note #1 on NASA Grant NsG-702
Series 6
Issue 17
May, 1965

ABSTRACT

13642

The study is concerned with the dynamic properties of an explosion in a medium consisting of condensed phase fuel particles dispersed in a gaseous oxidizer. The influence of the parameters which characterize the problem is determined from numerical solutions of a simplified analytical model and the effect of transport phenomena on equilibrium gas-particle dynamics is examined.

The history of the process is analyzed assuming that the flow field is one-dimensional in space. While the most realistic approach is adopted for the thermodynamic description of the medium, all other effects are simplified to the most elementary form in order to establish a fundamental point of departure for the assessment of their possible influence. The flow field is considered to consist of a simple wave where the oxidizer gas carrier is compressed, and of a reaction zone where the substance acquires the state of thermodynamic equilibrium. At first two extremes of particle motion in the compression wave are taken into account: (I) when they are assumed to be stationary at all times; (II) when they are supposed to follow the gas motion identically. Then the effects of a more realistic particle motion are investigated. The solutions, obtained by the use of an IBM 7090 computer, refer to the properties of a hydrazine spray in oxygen initially at NTP, and use the initial loading factor (ratio of particle to gas concentrations) and the relative combustion front velocity as the major parameters of the problem.

Author

Both the transient process and the final steady state are determined for a wide range of these parameters.

ACKNOWLEDGMENT

This research was supported by the National Aeronautics and Space Administration under Grant NsG-702.

The author extends his sincere appreciation to the staff of the Propulsion Dynamics Laboratory for their cooperation, especially to Ronald Panton and Daniel Schlosky, to MacKenzie Patterson for his diligent preparation of the figures, and to Kenneth Hom and Walter Giba for their assistance in obtaining the experimental record in Figure 1-1.

CONTENTS

FIGURE CAPTIONS

Fig. 1-1 Explosion in the Time-Space Domain. On the left a self-light streak photograph of the development of explosion of a kerosine spray in oxygen ignited by a glow-plug in a 2 inch diameter tube; on the right the corresponding wave diagram.

2-1 Solution in the Time-Space Domain for $\eta_c = .1$ and $S = .2$ while particles follow gas motion identically (case (II))

2-2 World Lines of the Reaction Front

2-3 Pressure Pulses

2-4 Transient Process in the Pressure-Temperature Plane

2-5 Transient Process on the Pressure-Specific Volume Plane

2-6 Steady-State Parameters on the Pressure-Specific Volume Plane

2-7 Steady-State Parameters on the Pressure-Temperature Plane

2-8 Steady State with Shock Compression

3-1 Influence of Particle Motion in the Time-Space Domain

3-2 Influence of Particle Motion in the Pressure-Time Plane for $C_D(Re)$ as well as constant values of C_D.

3-3 Particle Acceleration at the Reaction Front vs. Time

3-4 Drag Coefficient at the Reaction Front vs. Time

3-5 Reynolds Number at the Reaction Front vs. Time

3-6 Effect of Particle Size on the Pressure Overshoot, $S = .2$.

NOMENCLATURE

Dimensional

a - velocity of sound

d - particle diameter

c_p - constant pressure specific heat

c_v - constant volume specific heat

e - internal energy per unit mass (including internal energy of formation)

h - enthalpy per unit mass (including enthalpy of formation)

g - Gibbs free energy per unit mass (including energy of formation)

K - constant describing the rate of decrease of the surface area of the reacting fuel particles

$\dot{m}$ - time rate of change of mass per unit cross-section area

$\mathcal{M}$ - molar mass

n - particle number density

p - pressure

r - particle radius

$\bar{r}$ - mean particle radius

$\mathcal{R}$ - universal gas constant

s - relative velocity of the reaction front

t - time

$t_o = r_o^2/K$

T - temperature

u - mass velocity

v - specific volume

w - absolute reaction front velocity

X - space coordinate of reaction front

y - concentration

λ - viscosity

ξ - particle trajectory in $t-X$ space

ρ - density

Subscripts

eq - equilibrium

f - fuel

fz - frozen

g - gas

go - initial gas properties

gr - gas properties in the reaction zone

gx - gas properties immediately ahead of the reaction front

m - mixture

mo - initial mixture properties

o - initial conditions

p - particle

po - initial particle properties

pr - particle properties in the reaction zone

px - particle properties immediately ahead of the reaction front

r - reaction zone properties

x - properties immediately ahead of the reaction front

s - steady state or entropy

ts - transient quantity defined by Eq. (2-76)

v - vapor

Superscripts

$*$ - Properties at the initial pressure

Non-dimensional

$A = a/a_o$

A_i, B_i - coefficients defined by Eqs. (2-45)

$C_p = c_p/(\frac{pV}{T})_{go}$

$\overline{C}_p = c_p/(\frac{pV}{T})_{mo}$

C_D - drag coefficient

$D = \rho/\rho_{go}$

$E = e/(pv)_{go}$

F, G - coefficients defined by Eqs. (2-48)

$H_v = (h_v - h_c)/(RT/m_v)$

$\mathcal{H} = h/(pv)_{mo}$

$M = u_o/a_{go}$

$\overline{M} = u_o/a_{mo}$

$\widetilde{M} = u_o/(pv)_{go}$

$R = \bar{r}/\bar{r}_o$

Re - Reynolds number

$S = s/a_{go}$

$U = u/a_{go}$

$\widetilde{U} = u/(pv)_{go}$

$V = v/v_{go}$

$\overline{V} = v/v_{mo}$

$W = w/a_{go}$

$X = x/(a_{go}t_o)$

$Y = (y_{fuel\ burned})/(y_{oxidizer\ gas})$

z - moles per mole of gas plus vapor

γ - specific heat ratio of gas component

δ - condensed component constant pressure specific heat divided by that of the gaseous component

$\eta = \frac{\gamma_{particles}}{\gamma_{gas}}$ - loading factor

$\eta' = \frac{\gamma_{component\ in\ condensed\ phase}}{\gamma_{gaseous\ component}}$

$\Theta = T/T_o$

$\mu = \dot{m}_+/(\rho a)_{go}$

ν - volumetric fraction

$\bar{H} = \xi/(a_{go} t_o)$

σ - ratio of molecular weights

$\tau = t/t_o$

τ_{lag} - non-dimensional time lag

φ - fraction of particle mass still existing at time t out of that which entered the reaction zone at time t_x, defined by Eq. (2-27)

ϕ_1, ϕ_2, ϕ_3 - source terms defined by Eqs. (2-46)

γ - coefficient defined by Eq. (2-79)

1. INTRODUCTION

The study is concerned with the generation of pressure waves by the combustion of a heterogeneous medium consisting of fuel in the form of condensed phase particles dispersed in a gaseous oxidizer. The process under study is illustrated in Fig. 1-1, which represents, on the left, a self-light streak photograph of the development of an explosion of a kerosine spray in oxygen, ignited by a glow plug in a 2 inch square cross-section tube. While the acceleration of the combustion front is quite evident in such a record, the flow field ahead of it is not visible, although the existence of pressure waves is apparent from the wavy traces of particles within the expanding combustion zone.

The analysis deals with the initial stage of the process. Its extent in the time-space domain of Fig. 1-1 is restricted to the regime delineated there by the broken line, indicating that the scope of study is in essence limited to the interval when the process is not yet affected by any wave interaction phenomena. The flow field under consideration is represented by the wave diagram on the right side of Fig. 1-1, demonstrating the characteristics of the compression wave ahead of the flame, as well as those in the reaction zone. The gas motion is represented by broken lines, while a particle trajectory is displayed by a dotted line.

The purpose of this work is to lay down the fundamental background for a systematic study of the flow field of Fig. 1-1. In the development of the theory, care has been taken to introduce all basic concepts in a general form so that a more accurate description of the problem could be accommodated later.

In order to assess the relative importance of the variety of physical effects that can be taken under consideration, it appeared most reasonable to take into account at first the most realistic description of the thermodynamic properties of the medium, and simplify all other effects to the most elementary form, permitting the establishment of bounds for the extent of their possible influence. In this connection, the treatment of the problem has been simplified by the introduction of the following idealizations:

1. The medium consists of fuel particles in a condensed phase, and of a gaseous oxidizer in which they are uniformly dispersed. The size of the particles is assumed expressible in terms of a single, representative radius, while their number is virtually invariant, and the volumetric fraction they occupy is negligible.

2. The flow field is comprised of a simple wave, where the oxidizer gas carrier is compressed while the change in phase or state of fuel particles is negligible, and of a reaction zone varying with time, where the product gas is at a spatially uniform state while the particles acquire a distribution in size depending on the time of their arrival in this zone. As illustrated by the somewhat idealized wave diagram of Fig. 1-1, one

of the consequences of this idealization is the substitution of a set of horizontal lines for the system of characteristics in the reaction zone. The approximation resulting from this simplification, as demonstrated on this diagram, ought to be quite good.

3. Two extremes of particle motion in the compression wave are considered:

Case (I) where they are assumed at rest, and

Case (II) where they are supposed to follow the gas motion identically.

4. In the compression wave the gaseous substance is assumed to behave as a perfect gas with constant specific heats, while in the reaction zone its thermodynamic properties are determined from equilibrium composition analysis that takes into account the distribution of fuel particles, as pointed out in Idealization 2.

5. While algebraically the problem is formulated in such manner that any law for the reaction rate, as well as for the relative speed of the combustion front, could be accommodated, the numerical solutions are obtained for the commonly accepted rule of a constant rate of decrease in the surface area of fuel particles (whose validity has been established experimentally only for the case of a single droplet burning in a stagnant atmosphere) and a constant, relative velocity of the front relative to the gas phase which has been adopted as one of the major parameters for the study.

6. For numerical solutions the combustion front is considered to act solely as an interface between the reaction zone and the unreacted medium without exhibiting any change in pressure, and all extraneous effects, pertinent in particular to liquid sprays, such as particle size and concentration profiles, vaporization and shattering (in compliance with Idealization 1), turbulence, transverse motion, boundary layer, and heat transfer phenomena, are neglected.

After examining the relative importance of the various parameters of the problem by the above method, the influence of particle motion on the development of the flow field is investigated. This is accomplished by assigning a realistic acceleration force to the particles ahead of the reaction front while retaining the simple wave form for the gas flow field.

Finally, the influence that heat and mass transfer between phases may exert on the gas wave dynamic processes is studied. The results of this study serve to estimate the importance of transport phenomena in the unreacted region on the prominent wave processes in a two-phase system.

Relationship to Current Literature

As a result of its profound influence upon the performance analysis of rocket engines under both steady and unsteady operating conditions, the fluid dynamics of gases containing suspensions of small particles has become recently a subject of intensive study. The physical relations governing the motion of a gas containing non-interacting solid particles have been

formalized by Marble [1] who, besides uniform flow conditions, examined also the boundary layer flow and the Prandtl-Meyer expansion. The relaxation phenomena behind shock and rarefaction waves propagating through a particle-laden gas have been studied by Soo [2], Kriebel [3], and Rudinger [4, 5], while the one-dimensional expansion of gas particle systems was analyzed by Soo [2] and Kliegel [6]. Rudinger [7] also investigated the effects of finite particle volume on particle-gas dynamics and hence determined the range of validity for the commonly accepted assumption that the particle volume is negligible. Williams [8, 9] considered more specifically gas-liquid droplet systems, inquiring into the characteristic features of spray deflagration, as well as the structure of two-phase detonation waves. A comprehensive exposition of two-phase combustion theory, as well as a thorough review of the literature, is given by Williams [10] in his text on combustion.

With the aim of contributing toward a better understanding of combustion instability phenomena in liquid propellant rocket engines, the group at Princeton under the direction of Crocco has carried out a comprehensive program of study on the subject with a particular consideration of acoustic phenomena [11, 12, 13, 14], as well as non-linear wave interactions [15] and the influence of acoustic oscillations in the ambient gas on single droplet burning [16]. Agosta's group, meanwhile, investigated the propagation of pressure waves in chemically reactive two-phase mixtures [17] and the effect of various droplet phenomena on heterogeneous combustion [18]. All these studies, however, have been concerned primarily with the determination of conditions

which would contribute toward the amplification of an input pressure disturbance without inquiring into the mechanism of its initial growth.

The initial build-up of a pressure pulse in gaseous combustion is now quite well understood [19, 20, 21]. The corresponding process in a heterogeneous medium has been taken for granted by most of the investigators although its proper understanding and control may yield one of the most effective means of suppressing the tendency toward unstable operation of a combustion chamber.

2. GENERATION OF PRESSURE WAVES

2-1. Analysis

2-1.1. State Parameters

The state of the substance is described in terms of pressure, temperature, and composition as independent parameters. All other thermodynamic functions are then evaluated by the use of fundamental thermodynamic identities for equilibrium composition on the basis of known properties of each constituent. The composition is described in terms of volumetric fractions, $\mathcal{V}_i$, and concentrations, y_i (in units of mass per unit of space).

The particles are described, according to Idealization 1, by means of a representative radius, so that the volumetric fraction they occupy is given by

$$\mathcal{V}_p = \frac{4}{3}\pi \bar{r}^3 n \tag{2-1}$$

where

$$\bar{r}^3 = \frac{1}{n}\int_0^\infty r^3 f(r)\, dr$$

and

$$n = \int_0^\infty f(r) dr$$

is the particle number density.

Their concentration is then:

$$y_p = \rho_p \mathcal{V}_p = \frac{4}{3}\pi \rho_p \bar{r}^3 n \tag{2-2}$$

A corresponding expression can be written for the gaseous phase.

The initial loading factor of the mixture is, under such circumstances,

$$\varkappa_0 \equiv \left(\frac{y_{particles}}{y_{gas}}\right)_0 \tag{2-3}$$

where subscript "o" denotes the initial state.

The composition of the gas in the reaction zone is described in terms of the mass ratio

$$Y_r \equiv \frac{y_{fuel\ burned}}{y_{oxidizer\ gas}} \tag{2-4}$$

whence its rate of change

$$\frac{dY_r}{dt} = \frac{1}{y_{oxidizer\ gas}}\left(\frac{dy_{fuel\ burned}}{dt} - Y_r \frac{dy_{oxidizer\ gas}}{dt}\right) \tag{2-5}$$

At the same time in terms of the average concentration of the gas in the reaction zone, y_{gr},

$$y_{fuel\ burned} + y_{oxidizer\ gas} = y_{gr} \tag{2-6}$$

The front travels at a relative velocity S with respect to the oxidizer gas and since the gas is admitted to the reaction zone only by the action of the front of this zone when the local gas concentration is y_{gx},

$$\frac{d}{dt}\left(\chi_r y_{oxidizer\ gas}\right) = \varsigma y_{gx} \tag{2-7}$$

while, as is readily recognized,

$$\frac{d}{dt}\left(X_r y_{\text{fuel burned}}\right) = \dot{m}_f \tag{2-8}$$

where $\dot{m}_f$ is the rate of gas generation due to the combustion of fuel per unit area.

With Eqs. (2-4), (2-6), (2-7), and (2-8), Eq. (2-5) becomes

$$\frac{d\bar{Y}}{dt} = \frac{1+\bar{Y}_r}{y_{gr} X_r}\left(\dot{m}_f - s\, y_{gx} \bar{Y}_r\right) \tag{2-9}$$

2-1.2. Fundamental Relations

The variation with time of the state in the reaction zone is prescribed by means of a series of conservation equations. The equations for the conservation of mass and energy are presented for the mixture, the gas, and the particles in this region to illustrate the consistency of the development although they will not all be used in the analysis. The energy relations take into account the energy expended by the compression process of the pressure wave whose action forms the central subject of the analysis. The source terms in the principal conservation equations depend on the gas generation rate which in turn is determined from the particle continuity equation that is subject to a given expression for the rate of particle consumption by the reaction process.

The continuity equation for the mixture in the reaction zone states that the mass per unit cross-sectional area increases at a rate equal to the sum of the oxidizer and particle flux across the front,

$$\frac{d}{dt}\left(y_{gr}\chi_r + m_{pr}\right) = S\,y_{g\chi} + \dot{m}_{p\chi} \qquad (2\text{-}10)$$

where m_{pr} is the particle mass in the reaction zone and $\dot{m}_{p\chi}$ is the flux of particles into the reaction zone at time t.

Since gas is generated in the reaction zone at the expense of particles, the continuity equation for the gas is in essence the derivative of Eq. (2-6), so that, in accordance with Eqs. (2-7) and (2-8), it is represented by the relation

$$\frac{d}{dt}\left(y_{gr}\chi_r\right) = \dot{m}_f + S\,y_{g\chi} \qquad (2\text{-}11)$$

The particle continuity equation is then obtained by subtracting Eq. (2-11) from Eq. (2-10):

$$\frac{d}{dt}\left(m_{pr}\right) = \dot{m}_{pr} = \dot{m}_{p\chi} - \dot{m}_f \qquad (2\text{-}12)$$

The energy equation for the mixture in the reaction zone specifies that the internal energy accumulates there as the result of the influx of material across the combustion front and flow work on the system, while it is expended in the form of work performed by the expanding front on the compression of the medium by the simple wave, that is

$$\frac{d}{dt}\left(y_{gr}e_{gr}\chi_r + m_{pr}e_{pr}\right) = y_{g\chi}S\left(e_{g\chi} + \frac{p_\chi}{\rho_{g\chi}}\right) + \dot{m}_{p\chi}\left(e_{p\chi} + \frac{p_\chi}{\rho_{p\chi}}\right) \qquad (2\text{-}13)$$

where e denotes the internal energy which includes the energy of formation, and subscripts pr and $p\chi$ refer to particle quantities in the reaction zone and just ahead of the front, respectively.

The mass transfer in the reaction zone from the particles to the gas is associated with an energy transfer, $\dot{m}_f\left(e_{pr}+\frac{p_r}{\rho_{pr}}\right)$, so that the gas and particle energy equations are

$$\frac{d}{dt}\left(y_{gr}e_{gr}x_r\right)=y_{gx}s\left(e_{gx}+\frac{p_x}{\rho_{gx}}\right)+\dot{m}_f\left(e_{pr}+\frac{p_r}{\rho_{pr}}\right) \qquad (2\text{-}14)$$

and

$$\frac{d}{dt}\left(y_{pr}e_{pr}x_r\right)=\dot{m}_{px}\left(e_{px}+\frac{p_x}{\rho_{px}}\right)-\dot{m}_f\left(e_{pr}+\frac{p_r}{\rho_{pr}}\right) \qquad (2\text{-}15)$$

Equations (2-9) through (2-15) hold for any thermodynamic description and for a general mass generation rate. However, according to Idealization 1, $y_p \ll 1$, so that $y_g \approx 1$, $\rho_g \approx y_g$, and $\rho_p \gg y_p$, while from Idealization 2, ρ_p = const. Consequently, only the mass and energy equations for the gas phase and the mass equation for the particles are needed for determining the generation of pressure waves at the combustion front. Equations (2-9), (2-11), and (2-14) become respectively:

$$\frac{dY_r}{dt}=\frac{1+Y_r}{\rho_{gr}x_r}\left(\dot{m}_f-s\rho_{gx}Y_r\right) \qquad (2\text{-}16)$$

while

$$\frac{d}{dt}\left(\rho_{gr}x_r\right)=\dot{m}_f+s\rho_{gx}$$

or

$$\frac{d\ln\rho_{gr}}{dt}=\frac{1}{x_r}\left(\frac{\dot{m}_f+s\rho_{gx}}{\rho_{gr}}-\omega_x\right) \qquad (2\text{-}17)$$

where

$$\omega_x = \frac{dx_r}{dt}$$

and

$$\frac{d}{dt}\left(\rho_{gr} e_{gr} x_r\right) = \dot{m}_f e_{pr} + s\rho_{gx}\left(e_{gx} + \frac{p_x}{\rho_{gx}}\right) - p_x \omega_x$$

or

$$\frac{de_r}{dt} = \frac{1}{\rho_{gr} x_r}\left[\dot{m}_f(e_{pr} - e_{gr}) + s\rho_{gx}(e_{gx} - e_{gr}) - p_x u_{gx}\right] \quad (2\text{-}18)$$

where

$$u_{gx} = \omega_x - s$$

is the absolute gas velocity at the instant when it is overtaken by the reaction front.

As a consequence of the fact that, as pointed out at the outset of this section, the state of the products in the reaction zone are described in terms of p_r, T_r, and Y_r, it follows that

$$\rho_{gr} = \rho_{gr}(p_r, T_r, Y_r) \quad , \quad e_{gr} = e_{gr}(p_r, T_r, Y_r)$$

and Eqs. (2-17) and (2-18) can be written more explicitly as follows:

$$\frac{\partial \ln \rho_{gr}}{\partial \ln p_r}\frac{d\ln p_r}{dt} + \frac{\partial \ln \rho_{gr}}{\partial \ln T_r}\frac{d\ln T_r}{dt} + \frac{\partial \ln \rho_{gr}}{\partial Y_r}\frac{dY_r}{dt} = \frac{1}{x_r}\left(\frac{\dot{m}_f + s\rho_{gx}}{\rho_{gr}} - \omega_x\right) \quad (2\text{-}19)$$

and

$$\frac{\partial e_{gr}}{\partial \ln p_r}\frac{d\ln p_r}{dt} + \frac{\partial e_{gr}}{\partial \ln T_r}\frac{d\ln T_r}{dt} + \frac{\partial e_{gr}}{\partial Y_r}\frac{dY_r}{dt} = \frac{1}{\rho_{gr} x_r}\left[\dot{m}_f(e_{pr} - e_{gr}) + s\rho_{gx}(e_{gx} - e_{gr}) - p_x u_{gx}\right] \quad (2\text{-}20)$$

where according to thermodynamic identities

$$\frac{\partial e}{\partial \ln p} = \frac{p}{\rho}\left(\frac{\partial \ln \rho}{\partial \ln T} + \frac{\partial \ln \rho}{\partial \ln p}\right)$$

and

$$\frac{\partial e}{\partial \ln T} = c_p T + \frac{p}{\rho}\frac{\partial \ln \rho}{\partial \ln T}$$

while, as a consequence of Idealization 2, $e_{px} = e_{pr} = e_{po} = \text{const.}$

The compression process, which yields the expressions for $\rho_{gx}(p_x)$, $e_{gx}(p_x)$, and $u_{gx}(p_x)$, is accomplished, according to Idealization 2, by the action of a simple wave which, as stated in Idealization 4, propagates through a perfect gas with constant specific heats. Consequently:

$$\rho_{gx} = \rho_{go}\left(\frac{p_x}{p_o}\right)^{1/\gamma}$$

$$e_{gx} = e_{go} + \frac{1}{\gamma - 1}\frac{p_o}{\rho_{go}}\left[\left(\frac{p_x}{p_o}\right)^{\frac{\gamma-1}{\gamma}} - 1\right] \qquad (2\text{-}21)$$

and

$$u_{gx} = \frac{2}{\gamma - 1} a_{io}\left[\left(\frac{p_x}{p_o}\right)^{\frac{\gamma-1}{2\gamma}} - 1\right]$$

where a_{io} is the velocity of sound in the undisturbed medium. Its value depends on the assumption concerning the particle motion. In this respect, as stipulated in Idealization 3, two cases are considered: (I) where the particles do not participate in the gas motion at all, and (II) when they follow the gas motion identically.

In case (I) then:

$$a_{Io} = \sqrt{\gamma \frac{R}{m_{go}} T_o} = a_{go} \qquad (2\text{-}22)$$

since disturbances are propagated only through the gas.

In case (II), however, the particles are an integral part of the mixture, so that its molar mass becomes, according to Eq. (2-3), $\mathcal{M}_m = \mathcal{M}_{g_0}(1+\eta_0)$; and

$$a_{II_0} = \sqrt{\gamma \frac{\mathcal{R}}{\mathcal{M}_{g_0}(1+\eta_0)} T_0} = \frac{a_{g_0}}{\sqrt{1+\eta_0}} \tag{2-23}$$

The quantity γ is the specific heat ratio of the gas phase.

The mass generation rate, the last quantity needed to complete the formulation of the problem, is evaluated as follows. The mass of particles accumulated in the reaction zone per unit cross-section area over the total time interval from o to t is

$$m_{pr} = \int_0^t \dot{m}_{px}(t_x)\, \varphi(t, t_x)\, dt_x \tag{2-24}$$

where $\varphi(t, t_x)$ is the fraction of particle mass still existing at time t out of that which entered the reaction zone at time t_x. From Eq. (2-24) then:

$$\dot{m}_{pr} = \frac{d}{dt}\int_0^t \dot{m}_{px}(t_x)\varphi(t,t_x)dt_x = \int_0^t \dot{m}_{px}(t_x)\frac{d\varphi(t,t_x)}{dt}dt_x - \dot{m}_{px}(t)\varphi(t,t) \tag{2-25}$$

and Eq. (2-12) yields

$$\dot{m}_t = -\int_0^t \dot{m}_{px}(t_x)\frac{d\varphi(t,t_x)}{dt}dt_x + \dot{m}_{px}(t_x)\left[1-\varphi(t,t)\right] \tag{2-26}$$

The quantity $\varphi(t, t_x)$ can be expressed in terms of concentrations averaged over the whole extent of the reaction zone, $\bar{y}_{pxr}(t, t_x)$. Consequently, with the use of Eq. (2-2),

$$\varphi(t,t_x) = \frac{\bar{y}_{pxr}(t,t_x)\, X_r(t)}{\bar{y}_{pxr}(t_x,t_x)\, X_r(t_x)} = \frac{\bar{r}^3(t,t_x)\,\bar{n}_{pxr}(t,t_x)\,X_r(t)}{\bar{r}^3(t_x,t_x)\,n_{pxr}(t_x,t_x)\,X_r(t_x)} \tag{2-27}$$

where $\bar{n}_{p\chi r}(t,t_\chi)$ is the average number density of those particles which entered the reaction zone at time t_χ and still exist at time t (i.e., in our case their number at time t divided by the width of the reaction zone at the same time). But, as stipulated by Idealization 1, their number $n_{p\chi r}(t,t_\chi)\,\chi_r(t)$ is invariant, so that

$$\left.\begin{aligned} \varphi(t,t_\chi) &= \frac{\bar{r}^3(t,t_\chi)}{\bar{r}^3(t_\chi,t_\chi)} \\ \text{whence} \\ \varphi(t,t) &= 1 \\ \text{and} \\ \frac{d\varphi(t,t_\chi)}{dt} &= \frac{3}{\bar{r}^3(t_\chi,t_\chi)}\,\bar{r}^2(t,t_\chi)\,\frac{d\bar{r}}{dt} \end{aligned}\right\} \qquad (2\text{-}28)$$

Furthermore, since according to Idealization 2 at $t = t_\chi$ the particles are still intact, it follows that $\bar{r}(t_\chi,t_\chi) = \bar{r}_o$.

Consequently Eq. (2-26) becomes

$$\dot{m}_f = -\frac{3}{\bar{r}_o^3}\int_o^t \dot{m}_{p\chi}(t_\chi)\,\bar{r}^2(t,t_\chi)\,\frac{d\bar{r}}{dt}\,dt_\chi \qquad (2\text{-}29)$$

Equation (2-29) attains an explicit form by the introduction of an expression for the rate of particle consumption. For this purpose, as specified in Idealization 5, the commonly accepted rule

$$\frac{d\bar{r}}{dt} = -\frac{K}{\bar{r}} \qquad (2\text{-}30)$$

has been adopted. Equation (2-29) reduces then to

$$\dot{m}_t = \frac{3K}{\bar{r}_o^3} \int_0^t \dot{m}_{p\lambda}(t_\lambda)\, \bar{r}(t, t_\lambda)\, dt_\lambda \qquad (2\text{-}31)$$

where

$$\left.\begin{aligned} \bar{r}_c(t, t_\lambda) &= \left(\bar{r}_c^2 - 2K[t - t_\lambda]\right)^{1/2}, \quad t - t_\lambda \leq \frac{\bar{r}_c^2}{2K} \\ &= 0 \qquad\qquad\qquad\quad , \quad t - t_\lambda \geq \frac{\bar{r}_c^2}{2K} \end{aligned}\right\} \qquad (2\text{-}32)$$

Finally, since in case (I) the particles remain stationary and therefore enter the reaction zone only by being swept over by its front:

$$\dot{m}_{p\lambda}(t_\lambda) = \eta_o \rho_{go} \omega_\lambda(t_\lambda) \qquad \text{for case (I)} \qquad (2\text{-}33)$$

while in case (II) they maintain a constant loading fraction in the compression wave, so that

$$\dot{m}_{p\lambda}(t_\lambda) = \eta_o S \rho_{g\lambda}(t_\lambda) \qquad \text{for case (II)} \qquad (2\text{-}33a)$$

2-1.3. Non-dimensional Formulation

As a consequence of the rule of Eq. (2-30), adopted here for the rate of particle consumption, the most natural standard for the reduction of the physical dimensions of the problem is the time constant:

$$t_o \equiv \frac{\bar{r}_c^2}{K} \qquad (2\text{-}34)$$

which, as is apparent from Eq. (2-32), expresses the double-life time of particles in the reaction zone.

Consequently the non-dimensional time and space coordinates are

$$\tau \equiv \frac{t}{t_c} \quad \text{and} \quad X \equiv \frac{x}{a_{g_0} t_c} \tag{2-35}$$

the latter being compatible with non-dimensional velocities

$$S \equiv \frac{s}{a_{g_0}}, \quad W_\lambda \equiv \frac{w_\lambda}{a_{g_0}}, \quad U_{g\lambda} \equiv \frac{u_{g\lambda}}{a_{g_0}} \tag{2-36}$$

The thermodynamic parameters are non-dimensionalized by referring them simply to the initial state of the undisturbed medium, i.e.,

$$P \equiv \frac{p}{p_0}, \quad \Theta \equiv \frac{T}{T_c}, \quad D \equiv \frac{\rho_g}{\rho_{g_0}}, \quad V \equiv D^{-1}, \quad C_p \equiv \frac{c_p \rho_{g_c} T_c}{p_c}, \quad E \equiv \frac{e \rho_{g_c}}{p_c} \tag{2-37}$$

Finally, the mass generation parameter and the radius are reduced in the straightforward manner by the introduction of

$$\mu \equiv \frac{\dot{m}_s}{(\rho a)_{g_0}} \quad \text{and} \quad R \equiv \frac{r}{r_c} \tag{2-38}$$

Since the problem is concerned specifically with the determination of the change of state in the reaction zone, its parameters become the major dependent variables, and, as a consequence of Idealization 2, they are functions of τ only, while X is relegated solely to the description of the extent

of the reaction zone and is therefore also a function of τ. Hence subscript gr is dropped everywhere without introducing any ambiguity, with the clear understanding that all symbols without any subscript refer solely to the gas in the reaction zone.

Under these circumstances Eqs. (2-19) and (2-20) become respectively:

$$A_1 \frac{d\ln P}{d\tau} + B_1 \frac{d\ln \Theta}{d\tau} = \bar{\Phi}_1 \tag{2-39}$$

and

$$A_2 \frac{d\ln P}{d\tau} + B_2 \frac{d\ln \Theta}{d\tau} = \bar{\Phi}_2 \tag{2-40}$$

or:

$$\frac{dP}{d\tau} = P \frac{B_2\bar{\Phi}_1 - B_1\bar{\Phi}_2}{A_1 B_2 - A_2 B_1} \tag{2-41}$$

and

$$\frac{d\Theta}{d\tau} = \Theta \frac{A_1\bar{\Phi}_2 - A_2\bar{\Phi}_1}{A_1 B_2 - A_2 B_1} \tag{2-42}$$

Equation (2-9) gives simply

$$\frac{dY_r}{d\tau} = \bar{\Phi}_3 \tag{2-43}$$

while from the definition of ω_x,

$$\frac{dX}{d\tau} = W_x \tag{2-44}$$

The coefficients in these equations are defined as follows:

$$\left.\begin{aligned} A_1 &\equiv -\left(\frac{\partial \ln V}{\partial \ln P}\right)_{\theta,Y}, \qquad B_1 \equiv -\left(\frac{\partial \ln V}{\partial \ln \theta}\right)_{P,Y} \\ A_2 &\equiv \left(\frac{\partial E}{\partial \ln P}\right)_{\theta,Y} = PV(A_1 + B_1) \\ B_2 &\equiv \left(\frac{\partial E}{\partial \ln \theta}\right)_{P,Y} = C_p\theta + PVB_1 \end{aligned}\right\} \tag{2-45}$$

The source terms are given by

$$\bar{\Phi}_1 \equiv \frac{1}{X}\left[(\mu + SD_{gx})V - W_x\right] + F\bar{\Phi}_3 \tag{2-46}$$

$$\bar{\Phi}_2 \equiv \frac{V}{X}\left[\mu(E_{po} - E) + SD_{gx}(E_{gx} - E) - P_x U_{gx}\right] - G\bar{\Phi}_3 \tag{2-47}$$

where

$$F \equiv \left(\frac{\partial \ln V}{\partial Y}\right)_{P,\theta} \quad \text{and} \quad G \equiv \left(\frac{\partial E}{\partial Y}\right)_{P,\theta} \tag{2-48}$$

while

$$\bar{\Phi}_3 \equiv \frac{V}{X}\left(\mu - SD_{gx}Y\right)(1+Y) \tag{2-49}$$

and

$$W_x = S + U_{gx}(P_x) \tag{2-50}$$

Furthermore, as a consequence of Eqs. (2-21),

$$D_{gx} = P_x^{1/\gamma} \tag{2-51}$$

$$E_{gx} = E_{gc} + \frac{1}{\gamma-1}\left[P_x^{\frac{\gamma-1}{\gamma}} - 1\right] \tag{2-52}$$

and

$$U_{gx} = \frac{2}{\gamma-1}\left[P^{\frac{\gamma-1}{2\gamma}} - 1\right] \quad \text{for case (I)} \tag{2-53}$$

or

$$U_{gx} = \frac{2}{\gamma-1}\,\frac{P^{\frac{\gamma-1}{2\gamma}} - 1}{\sqrt{1+\eta_c}} \quad \text{for case (II)} \tag{2-53a}$$

Finally the gas generation parameter becomes, according to Eqs. (2-31), (2-33), and (2-38),

$$\mu = 3\eta_c \int_0^{\tilde{\tau}} W_x(P_x) R(\tau;\tilde{\tau}_x)\, d\tilde{\tau}_x \quad \text{for case (I)} \tag{2-54}$$

where $W_\lambda(P_\lambda)$ is determined by means of Eqs. (2-50) and (2-53), and, with the use of Eq. (2-51),

$$\psi = 3\tfrac{1}{2} S \int_0^{\tau} P_\lambda^{7/8} R(\tau, \tau_\lambda)\, d\tau_\lambda \quad \text{for case (II)} \tag{2-54a}$$

while, as a consequence of Eqs. (2-32), (2-34), and (2-38),

$$R(\tau, \tau_\lambda) = \left(1 - 2|\tau - \tau_\lambda|\right)^{1/2}, \quad |\tau - \tau_\lambda| \le \frac{1}{2}$$
$$= 0, \quad |\tau - \tau_\lambda| \ge \frac{1}{2} \tag{2-55}$$

The problem is now fully defined in terms of four differential equations, Eqs. (2-41), (2-42), (2-43), and (2-44), and one integral equation, Eq. (2-54), which describe the variation of five dependent variables: P, Θ, Y, X, and μ. The primary coefficients in these equations are evaluated from the thermodynamic equilibrium equation and state data giving in essence

$$V = V(P, \Theta, Y), \quad C_p = C_p(P, \Theta, Y) \quad \text{and} \quad E = E(P, \Theta, Y) \tag{2-56}$$

and the rest of the coefficients are, by virtue of Eqs. (2-51), (2-52), and (2-53), functions of P_λ only.

The integration is carried out subject to the following initial conditions:

$$P = \Theta = 1, \quad Y = X = \mu = 0 \quad @ \quad \tau = 0 \tag{2-57}$$

(while, as a consequence of Eqs. (2-56), $V = 1$ and $E = E_c$) and the constraint prescribed by Idealization 6:

$$P_x = P \tag{2-58}$$

for specific values of the loading factor, η_o, and the relative speed of the combustion front, S, which, in the formalism, became the major parameters of the study.

2-1.4. Steady State

For each set of parameters the solution approaches asymptotically a steady state that results from the vanishing of the three derivatives expressed by Eqs. (2-41), (2-42), and (2-43) while that of Eq. (2-44) becomes a constant, or, what amounts to the same, from the fact that all source terms vanish while W_x attains its steady-state limit. On the basis of Eqs. (2-46), (2-47), (2-49), and (2-50), the steady state is therefore defined in terms of the following relations:

$$[\mu_s + S D_{gx}] V_s - [S + U_{gx}] = 0 \tag{2-59}$$

$$\mu_s [E_{p_o} - E_s(P_s, V_s, Y_s)] + S D_{gx} [E_{g_x} - E_s(P_s, e_s, Y_s)] - P_s U_s = 0 \tag{2-60}$$

$$\mu_s - S D_{gx} Y_s = 0 \tag{2-61}$$

where subscript s refers to the steady state. It should be noted also that, as a consequence of Eqs. (2-56), V_s has been

adopted as an independent variable, replacing ϵ, so that E_s became a function of P_s, V_s, and γ_s, and, in accordance with the constraint of Eq. (2-58), it has been already taken into account that $P_\lambda = P_s$.

Equations (2-59) and (2-61) yield

$$V_s = \frac{1}{1+\gamma_s}\left[\frac{1}{D_{g\lambda}} + \frac{U_{g\lambda}}{S\, D_{g\lambda}}\right] \qquad (2\text{-}62)$$

while Eqs. (2-60) and (2-61) give

$$E_s(P_s, V_s, \gamma_s) = \frac{1}{1+\gamma_s}\left[E_{g\lambda} + E_{fo}\gamma_s - \frac{P_s U_{g\lambda}}{S\, D_{g\lambda}}\right] \qquad (2\text{-}63)$$

Equation (2-62) can be looked upon as representing a relationship between V_s and P_s, with γ_s and S as parameters. Of these, one can be eliminated by means of Eq. (2-63) to yield in effect expressions for lines of constant S or of constant γ_s in the $P_s - V_s$ plane. Moreover, as is readily evident from Eqs. (2-62) and (2-63), the elimination of $U_{g\lambda}$ causes the concomitant elimination of S, and, consequently, the disappearance of any dependence upon the motion of particles in the simple wave. Hence the relationship between the state parameters P_s, θ_s, and γ_s is independent of Idealization 3.

The steady-state gas generation term can be expressed directly from Eqs. (2-33) by noting that for $\dot{m}_{p\lambda} = 0$, as is apparent from Eq. (2-12), $\dot{m}_+ = \dot{m}_{p\lambda}$. It follows then that

$$\mu = \eta_o W_\lambda = \eta_o\left[S + U_{g\lambda}\right] \qquad \text{for case (I)} \qquad (2\text{-}64)$$

and

$$\mu = \eta_0 S D_{gx} \quad \text{for case (II)} \qquad (2\text{-}64a)$$

The same result is obtained, as the reader may amuse himself verifying, from Eqs. (2-54) and (2-55) with $P_x = P_s$ = const. and W_x = const.

Combining Eqs. (2-64) with Eq. (2-61), it follows that

$$Y_s = \frac{\eta_0 [S + U_{gx}]}{S D_{gx}} \quad \text{for case (I)} \qquad (2\text{-}65)$$

and

$$Y_s = \eta_0 \quad \text{for case (II)} \qquad (2\text{-}65a)$$

which permit lines of η_0 = const. to be plotted in the $P_s - V_s$ plane. Subsequently, by invoking Eqs. (2-56), lines of const. S, Y_s, and η_0 can be also plotted in the $P_s - \theta_s$ plane.

Since, as a rule, the simple wave will coalesce into a shock wave before the steady state is attained, it is also of interest to determine the steady-state parameters for the case of a shock wave followed by the reaction zone. This is accomplished quite simply with Eqs. (2-62), (2-63), and (2-65) by the use of normal shock relations for $D_{gx}(P_s)$, $E_{gx}(P_s)$, and $U_{gx}(P_s)$ in place of Eqs. (2-51), (2-52), and (2-53).

2-2. Results

2-2.1. Specifications

Numerical solutions were obtained by means of the University of California IBM 7090 computer with the use of JANAF Tables [22] as a source of data for the thermodynamic properties of the constituents. All the state parameters were determined for the equilibrium composition using our own program written for P, Θ, and Y as independent variables.

The particular mixture adopted for this purpose was liquid hydrazine and gaseous oxygen at an initial pressure of 1 atm and an initial temperature of 300° K (a_o = 330 m/sec). Since it turns out that for this mixture the mass of fuel is equal to the mass of the oxidizer at stoichiometric proportions, the value of $Y = 1$ corresponds to stoichiometric composition.

The value of the constant in Eq. (2-30) is for most hydrocarbons [23] about

$$K = 25 \times 10^{-4} \frac{cm^2}{sec}$$

so that the time constant defined by Eq. (2-34) is approximately

$$t_o = d_o^2 \quad \text{microseconds}$$

where d_o is the particle diameter in microns.

The parameters of the problems used for the computation of the transient behavior were

$$S = .05, \ .10, \text{ and } .20$$

and

$$\eta_o = .05, \ .10, \text{ and } .20$$

while for the final steady state a much wider scope of S from 0.005 to 0.2, Y from 0.005 to 1.6 (which, according to Eq. (2-65a), is equal to η_o in case (II)), and η_o from 0.005 to 0.2 has been explored.

2-2.2. Transient Process

The results for the transient case are expressed with reference to the steady state in terms of the following parameters:

$$X_{ts} \equiv \frac{X}{W_s} = \frac{K}{r_o^2} \frac{x_r}{u_s + s} \tag{2-66}$$

$$P_{ts} \equiv \frac{P-1}{P_s-1} = \frac{P-P_o}{P_s-P_o}; \quad V_{ts} \equiv \frac{V-1}{V_s-1} = \frac{\rho_s}{\rho} \frac{\rho-\rho_o}{\rho_s-\rho_o}; \quad \Theta_{ts} \equiv \frac{\Theta-1}{\Theta_s-1} = \frac{T-T_o}{T_s-T_o}$$

where subscript S refers to steady state. The use of these parameters enhances the correlation between the results and leads therefore to clearer conclusions.

To describe the general character of the solution, Fig. 2-1 has been plotted for a particular set of parameters $\eta_o = 0.10$ and $S = 0.20$ in case (II), i.e., when the particles follow the gas motion identically. The reaction front is represented by the thick continuous line, the thin lines describing the characteristics of the simple wave. Particle paths are shown by thin broken lines, the thick broken line delineating the end of reaction, i.e., when the particle radius becomes equal to zero. In accordance with Eq. (2-55), the residence time of each particle (until it disappears) in the reaction zone is 0.5. Since at $X = 0$ the particles are at rest, the intersect of the line denoting the end of the reaction zone with the τ-axis is

exactly 0.5; however, it is of interest to note that the transient is by no means over at that time.

Figure 2-2 describes the motion of the reaction front in the various cases investigated here. It should be noted that the front world-lines are depicted there in the reduced time-space coordinates where X_{ts} is used instead of the X of Fig. 2-1. To help decipher the diagrams, auxiliary curves of W_s as a function of S are inserted. In case (I), i.e., when the particles are at rest, both the increase in η_c and in S enhance the acceleration of the front. In case (II), however, just the opposite holds true, while the acceleration is always larger than in the previous case.

The corresponding pressure profiles are shown in Fig. 2-3. The trends of Fig. 2-2 are reflected here in the fact that cases of larger acceleration correspond to faster rise in pressure. The most significant, however, is the observation that it takes a surprisingly long time to attain steady state which, especially in case (I), none of the profiles achieved within the time interval well in excess of the double-life time of the particles. The steady state is attained most easily for low loading factors and low flame speeds in case (II), i.e., when the particles follow the motion of the gas identically. In drawing conclusions as to the absolute value of pressure, reference should be made, in accordance with Eq. (2-66), to the steady-state values (given in Figs. 2-6 and 2-7). One should note in this respect that a higher value of P_{ts} does not imply a higher value of P. In fact, as the reader may verify, higher pressures are developed

for the same value of η_o in case (I) than in case (II), although the opposite holds true for P_{ts} as it appears in Fig. 2-3.

Figure 2-4 demonstrates the relation between pressure and temperature, and Fig. 2-5 that between pressure and specific volume, over the whole range of the pressure pulse from the initial conditions when $P_{ts} = \theta_{ts} = V_{ts} = 0$ to the final steady state when $P_{ts} = \theta_{ts} = V_{ts} = 1$. They represent, in effect, integral curves of equations

$$\frac{dP}{d\theta} = \frac{P}{\theta} \frac{B_2\dot{\Phi}_1 - B_1\dot{\Phi}_2}{A_1\dot{\Phi}_2 - A_2\dot{\Phi}_1} \tag{2-67}$$

and

$$\frac{dP}{dV} = \frac{P}{\dot{\Psi}} \frac{B_2\dot{\Phi}_1 - B_1\dot{\Phi}_2}{A_1B_2 - A_2B_1} \tag{2-68}$$

where

$$\dot{\Psi} = \frac{V}{X}\left[W_x - (\mu + S D_x)V\right] \tag{2-69}$$

respectively. Equation (2-67) is obtained directly from Eqs. (2-41) and (2-42), while Eq. (2-68) is derived from Eq. (2-41) and the first term of Eq. (2-46) which, as can be verified by reference to Eq. (2-17), expresses the derivative: $-\frac{d\ln V}{d\tau}$.

Of particular interest here is the manner in which the steady state is approached. As it appears from Fig. 2-4, in case (I) the temperature tends to approach the steady state faster than pressure, producing even an overshoot for higher

loading factors and lower front velocities. For $\eta_0 = 0.05$, the pressure approaches the steady state earlier, and with $S = 0.20$, the temperature is then practically proportional to pressure. A similar role is played by $\eta_0 = 0.10$ and $S = 0.20$ in case (II), but the temperature overshoot is not apparent there within the scope of parameters used for our study. Figure 2-5, which in trend agrees of course with Fig. 2-4, shows a much more significant overshoot in specific volume, especially in case (I). In contrast to temperature, however, it occurs for both high loading factors and high front velocities.

2-2.3. Steady State

The steady-state diagrams which, as a consequence of the definitions of Eqs. (2-66), are necessary in order to decipher the results from Figs. 2-2 to 2-5, are given in Figs. 2-6 and 2-7, the former in the $P_s - V_s$ plane, and the latter in the $P_s - \theta_s$ coordinates. Plotted there are lines of constant Y_s besides lines of constant η_0 and S which appeared in the transient plots. For case (II), according to Eq. (2-65a), lines of const. Y_s and η_0 coincide with each other.

Finally, Fig. 2-8 gives the steady-state parameters in the $P_s - \theta_s$ plane when compression is assumed to be accomplished by a shock instead of the isentropic simple wave. By comparison with Fig. 2-7 it appears that the coalescing of the simple wave into shock has a relatively insignificant effect on the steady state attained by the pressure pulse.

2-3. Discussion and Conclusions

2-3.1. Salient Features of Solution

In order to bring out the essential character of the solution, it is instructive to examine the results under the assumption that the gas in the reaction zone behaves as a perfect gas with constant specific heat and the same molecular weight as the oxidizer. Hence, the volume ratio defined in terms of the pressure and temperature is

$$V = \Theta/P \tag{2-70}$$

and the energy, which applies only to lean mixtures, is

$$E = \frac{Y}{1+Y} E_{fg} + \frac{\Theta - 1}{\gamma_r' - 1} \tag{2-71}$$

The quantity E_{fg} is a constant energy of formation of stoichiometric products per unit mass of initial fuel particles at the initial state, and γ_r' is the constant specific heat ratio of the reaction zone gases. Consequently, Eqs. (2-45) become

$$\begin{aligned} A_1 &= 1 \quad , \quad B_1 = -1 \\ A_2 &= 0 \quad , \quad B_2 = \frac{\Theta}{\gamma_r' - 1} \end{aligned} \tag{2-72}$$

while Eqs. (2-48) yield

$$F = 0 \quad , \quad G = \frac{E_{fg}}{(1+Y)^2} \tag{2-73}$$

Substitution of Eqs. (2-46), (2-47), (2-49), (2-51), (2-52), (2-70), and (2-71) into Eqs. (2-41) and (2-42) and rearranging gives

$$\frac{dP}{d\tau} = \frac{\gamma_r - 1}{X}\left[\mu\left(\Omega + \frac{1}{\gamma_r - 1}\right) + \frac{\gamma_r - \gamma}{\gamma - 1}\frac{S}{\gamma_r - 1}(P - D_{gx}) - \frac{\gamma_r}{\gamma_r - 1} P U_{gx}\right] \quad (2\text{-}74)$$

and

$$\frac{d\theta}{d\tau} = \theta\frac{\gamma_r - 1}{X}\left[\frac{\mu}{P}\left(\Omega - \frac{\theta - 1}{\gamma_r - 1}\right) + \frac{S}{\gamma - 1}\left(1 - \frac{D_{gx}}{P}\right) - \frac{S(\theta - 1)D_{gx}}{(\gamma_r - 1)P} - U_{gx}\right] \quad (2\text{-}75)$$

where

$$\Omega \equiv E_{fo} - E_{fg} \quad (2\text{-}76)$$

is now an additional parameter of the problem.

It should be noted that Eqs. (2-43), (2-44), (2-54), and (2-74) do not contain any dependence on θ, and hence the pressure pulse may be solved independently of θ.

At the initial condition $\gamma_r = \gamma$ and $P = \theta = D_{gx} = 1$, and

$$\left(\frac{dP}{d\tau}\right)_{\tau=0} = (\gamma - 1)\left(\Omega + \frac{1}{\gamma - 1}\right)\underset{\tau \to 0}{\text{limit}}\frac{\mu}{X} \quad (2\text{-}77)$$

while

$$\left(\frac{d\theta}{d\tau}\right)_{\tau=0} = (\gamma - 1)\,\Omega \underset{\tau \to 0}{\text{limit}}\frac{\mu}{X} \quad (2\text{-}78)$$

For small values of τ, Eq. (2-54) can be represented approximately for both case (I) and case (II) as

$$\mu = 3\eta_0 S\tau \quad (2\text{-}79)$$

while X takes the form

$$X = 5\tau \tag{2-80}$$

which implies that the gas velocity is zero and that the particle size has not changed in the reaction zone. Hence, $\lim_{\tau \to 0} \frac{4}{X} = 3\eta_0$ and Eqs. (2-77) and (2-78) become

$$\frac{dP}{d\tau} = 3\eta_0(\gamma-1)\left(\Omega + \frac{1}{\gamma-1}\right) \tag{2-81}$$

and

$$\frac{d\Theta}{d\tau} = 3\eta_0(\gamma-1)\Omega \tag{2-82}$$

respectively. Note that at time zero, Eq. (2-49) is

$$\frac{dY}{d\tau} = 3\eta_0 \tag{2-83}$$

For the hydrazine fuel and oxygen gas considered in the analysis, $\Omega \approx 200$ while $\gamma = 1.4$. Hence, Eq. (2-81) is

$$\frac{dP}{d\tau} \approx 240\,\eta_0 \tag{2-84}$$

The discrepancy between values obtained from this expression and those from Figs. 2-3 and 2-7 arises primarily from the fact that V was not considered to be a function of Y in Eq. (2-66).

The steady-state solutions for a set of parameters are obtained by equating Eqs. (2-74) and (2-75) to zero with Eq. (2-61). Therefore,

$$\mu_s\left(\Omega + \frac{1}{\gamma_r-1}\right) = \frac{\gamma-\gamma_r}{\gamma-1}\frac{S(P_s - D_{gx})}{\gamma_r - 1} + \frac{\gamma_r}{\gamma_r-1} P_s U_{gx} \tag{2-85}$$

and

$$\frac{\mathcal{M}_s}{P_s}\left(\Omega - \frac{\theta_s - 1}{\gamma_r - 1}\right) = \frac{S(\theta - 1)}{\gamma_r - 1}\frac{D_{g\lambda}}{P_s} + U_{g\chi} - \frac{S}{\gamma - 1}\left(1 - \frac{D_{g\lambda}}{P_s}\right) \qquad (2\text{-}86)$$

With the help of Eq. (2-61), $\mathcal{M}_s$, S, and $U_{g\chi}$ may be eliminated from Eqs. (2-85) and (2-86) to yield a relation between the steady-state properties for a given Ω:

$$\theta_s = 1 + \frac{\gamma_r - 1}{1 + Y_s}\left[\frac{\gamma/\gamma_r}{\gamma - 1}\left(\frac{P_s}{D_{g\chi}} - 1\right) + \frac{Y_s}{\gamma_r}\left(\Omega - 1\right)\right] \qquad (2\text{-}87)$$

and hence

$$V_s = \frac{\theta_s}{P_s} = \frac{1}{P_s}\left[1 + \frac{\gamma_r - 1}{1 + Y_s}\left(\frac{Y}{\gamma_r}(\Omega - 1) - \frac{\gamma/\gamma_r}{1 + Y_s}\right)\right] + \frac{\gamma_r - 1}{1 + Y_s}\frac{\gamma/\gamma_r}{\gamma - 1}\frac{1}{D_{g\chi}} \qquad (2\text{-}88)$$

The solutions displayed in Figs. 2-7 and 2-8 indicate that the relationship between Y_s and θ is essentially independent of P. Hence the last term in the bracket of Eq. (2-87) dominates the first.

As in Fig. 2-6, Eq. (2-88) illustrates that for given values of Y_s and Ω the solutions for P_s and V_s lie approximately on a hyperbola.

2-3.2. Conclusions

As to overall conclusions, one may note the following consequences of our theory.

Most of the curves describing the transient process in Fig. 2-2 (especially for case (I)) are grouped together,

principally as a result of using $t_o = \frac{\bar{r}_o^2}{K}$ as reference time. It can be concluded, therefore, that the development of the transient process with time is governed essentially by the life time of particles which, in turn, depends only on the mean particle size and the reaction rate constant. As demonstrated in Figs. 2-4 and 2-5, the progress of the transient process on the thermodynamic plane depends, however, on the initial composition and on the relative velocity of the combustion front.

From Figs. 2-6 and 2-7, it appears that curves of constant are almost the same, independently of whether they refer to case (I) or case (II), while, as demonstrated from Eqs. (2-62) and (2-63), curves of const. $\ddot{Y}_s$ are identical. It follows therefore that, for the determination of the finally attained steady state, particle motion in the simple wave can be completely disregarded, provided that composition of the gas in the reaction zone, rather than the initial loading factor, is specified. At the same time, as far as this state is concerned, it is practically immaterial whether the compression process has been carried out by the simple wave on one side, or by a shock wave on the other side, of the whole spectrum of possible wave compression processes.

3. INFLUENCE OF PARTICLE MOTION

The need for more careful consideration of particle motion during the combustion initiation process is manifested by the wide variance in pressures obtained with case (I) and case (II) in the previous section. Consequently, the effects of such motion are here analyzed on the basis of a realistic drag law which requires the particle velocity in the unreacted region to depend not only on the gas velocity, but also on its acceleration. The flux of fuel into the reaction zone is a function of the velocity field. Hence, the feedback system, consisting of the reaction zone and the pressure fan, will be less stable, emphasizing the importance of the link between the chemico-kinetics and the gas dynamics of the problem.

Several important aspects of the solutions that will be obtained with real particle motion can be deduced immediately. The particle acceleration is zero at the start since it is generated by the flow field. The initial stage of the process is described, therefore, by case (I), while the motion of case (II) is approached at the final steady state because by definition there can be no velocity lag at the reaction front. Hence, conditions at the beginning and end of the transient are known from the results of case (I) and case (II) respectively, and the purpose of this section is to study the transition process.

Rudinger and Chang [5] presented the complete characteristic method of analysis for non-steady gas-particle mixture dynamics, together with several examples. Instead of applying their

sophisticated technique to this problem, it was decided to make several assumptions which render the problem more easily tenable and still permit the salient features of the phenomena to be determined.

3-1. Analysis

3-1.1. Particle Acceleration

Although the region ahead of the combustion front really consists of a complex wave region, it is assumed here that the flow field of the gas phase is described by the equilibrium simple wave of case (I), while the fuel particles again abide by Idealization 2 of section 2. The velocity field of the particles, on the other hand, is obtained by integrating the expression for the acceleration [5]:

$$\frac{Du_p}{Dt} = \frac{D^2\xi}{Dt^2} = \frac{3}{8} C_D \rho_g (u-u_p)|u-u_p| / (\bar{r}_o \rho_p) \qquad (3\text{-}1)$$

where u and u_p are the gas and particle velocity, ξ_p is a particle trajectory, $\frac{D}{Dt}$ is the substantial derivative in $t-x$ space, and C_D is the drag coefficient. The non-dimensional form of Eq. (3-1), consistent with the previous definitions of dimensionless time, space, velocity and density, is

$$\frac{DU_p}{D\tau} = \frac{D^2\Xi}{D\tau^2} = \frac{3}{8}\left(\frac{r_o a_{go}}{K}\right) C_D (U-U_p)|U-U_p| \frac{D_g}{D_p} \qquad (3\text{-}2)$$

where $\left(\frac{r_o a_{go}}{K}\right)$ is a non-dimensional parameter, $D_p \equiv \rho_p/\rho_{go}$ and $\Xi \equiv \xi/(t_o a_{go})$. The expression used for the drag coefficient, C_D,

is that proposed by Gilbert, Davis, and Altman [24]:

$$C_D = 28.\,Re^{-.85} + .48 \qquad (3\text{-}3)$$

where the Reynolds number, Re, is defined by

$$Re \equiv \frac{2\rho_g|u-u_p|\bar{r}_o}{\lambda} = \frac{2\,D_g|U-U_p|}{\Lambda} \qquad (3\text{-}4)$$

and λ is the gas viscosity, while $\Lambda \equiv \lambda/(\rho_{go} a_{go} \bar{r}_o)$.

In addition to Eq. (3-3), constant values of C_D were used to test the sensitivity of the solutions to the value of the drag coefficient.

3-1.2. Mass Generation Rate

Modifications to the analysis presented in the previous section due to the consideration of real particle motion occur only in the expression for the mass generation rate in the reaction zone, $\mathcal{M}$. Specifically, the expression for the flux of particles into the reaction zone at time t_x, m_{px} is needed. The general expression for this quantity, which applies here as well as to case (I) and case (II), is

$$\dot{m}_{px}(t_x) = y_{px}(\omega_x - u_{px}) = \eta_o \rho_{go} \frac{y_{px}}{y_{po}}(\omega_x - u_{px}) \qquad (3\text{-}5)$$

where y_{px} and u_{px} are the particle concentration and velocity just ahead of the reaction front at time t_x. The quantity u_{px} is obtained from Eq. (3-1), while the ratio $\frac{y_{px}}{y_{po}}$ is evaluated by integrating the negative of the divergence of the distance between two particle paths which pass on each side of the reaction front coordinates, (t, x). Substitution of Eq. (3-5)

into Eq. (2-26) yields the expression for the mass release rate, which, in non-dimensional form, is

$$\mu = 3\eta_o \int_o^{\tau} \frac{\gamma_{px}}{\gamma_{po}}(\tau_x)(W_x - U_{px})(\tau_x) R(\tau, \tau_x)\, d\tau_x \qquad (3\text{-}6)$$

3-1.3. Simple Wave Flow Field

The simple waves in the unreacted region will in general coalesce [25], which leads to triple-valued solutions for the gas velocity in the (t, x) plane. Since the particle velocity field depends directly on that of the gas, only single-valued solutions can be permitted. However, the shock wave would propagate approximately at the front of the cusp formed by the coalescence of the simple waves, so it was logical to use the solution corresponding to the largest value of $u(t, x)$ at those points (t, x) where the flow field was triple-valued. With this modification, the flow field of the particles can be computed in a straightforward manner.

The problem is now determined by the four differential equations from the previous section, Eqs. (2-36) through (2-39) and the integral equation, Eq. (3-6), which now replaces Eq. (2-49). The equations are subject to the same set of initial conditions and the various coefficients defined by Eq. (2-40) remain unchanged since they are state properties. The integration is then carried out subject to Eq. (2-51) for selected values of the loading factor, η_o, and the flame speed, S.

Before proceeding further, it is of interest to examine Eq. (3-2) more carefully. For $\frac{a_{go}\bar{r}_o}{K} = 0$, which corresponds to a zero transient period, the acceleration is zero for all τ since for any finite τ, t is zero, and hence the solution is given by case (I). However, for $\frac{a_{go}\bar{r}_o}{K} > 0$, the transient period will be greater than zero and the process will depend on the values of $\frac{a_{go}\bar{r}_o}{K}$, $\frac{r_o}{\lambda}$, and ρ_p. Therefore, the solutions for the $\lim\left(\frac{a_{go}\bar{r}_o}{K}\right) \to 0$ are different than when $\frac{a_{go}\bar{r}_o}{K}$ is set equal to zero.

3-2. Results

3-2.1. Specifications

In addition to η_o, the loading factor, and S, the flame speed, $\frac{a_{go}\bar{r}_o}{K}$, $\frac{r_o}{\lambda}$, and ρ_p are parameters of the problem because they appear in the expressions for the particle acceleration and drag coefficient, Eqs. (3-2) and (3-3) respectively. The values taken for a_{go}, λ, ρ_p, and K in this problem are

$$a_{go} = 330 \text{ m/sec} \quad (\text{oxygen, } 300^\circ\text{K})$$

$$\lambda = 2.03 \frac{\text{gm}}{\text{cm-sec}} \quad (\text{oxygen, } 300^\circ\text{K})$$

$$\rho_p = 1 \text{ gm/cc.} \quad (\text{hydrazine, } \sim 300^\circ\text{K})$$

$$K = .0025 \text{ cm}^2\text{/sec} \quad (\text{Godsave [23]})$$

while

$$\bar{r}_o = 6\tfrac{1}{4}, \ 25, \text{ and } 100 \text{ microns}$$

so that

$$\frac{a_{gc}\bar{r}_o}{K} = 8250,\ 33000,\ \text{and}\ 132000$$

and

$$\frac{\bar{r}_o}{\lambda} = 3.75,\ 12.30,\ \text{and}\ 49.20\ \frac{cm^2\text{-}sec}{gm}$$

The results were obtained for $\eta_o = .1$, since for this dilute case, the simple wave assumption for the gas phase in the unreacted region should be a good approximation.

3-2.2. Solutions

Figure 3-1 displays the solution in the $\tau - X$ plane for $S = .2$, and $\bar{r}_o = 25$ microns, and makes clear the assumptions regarding the simple wave flow field in the region of coalescence. The velocity lag of the particles is evident, and the effect of increased gas velocity on the particle acceleration may be observed by comparison of the two particle trajectories shown there.

The corresponding $P - \tau$ solution in Fig. 3-2 manifests the occurrence of a pressure overshoot during the transition from case (I) to case (II). This is due solely to the relationship between the gas-particle dynamics and the chemico-kinetics of the model without the consideration of any extraneous effects such as wave interactions and tube geometry. In addition, the solutions in Fig. 3-2 for constant C_D indicate that the overshoot will occur independently of the law assumed for the drag coefficient.

Figures 3-3, 3-4, and 3-5 give the acceleration, drag coefficient, and Reynolds number at the reaction front during the transient process and show that the particle is accelerated in essentially one unit of time, τ.

Figure 3-6 illustrates the dependence of the solution on $\bar{r}_o$ where the other parametric values are the same as in Figs. 3-1 through 3-5. Although the pressure peaks occur at about the same value of τ for the three particle sizes, this is not true in the dimensional time scale since $t = \frac{\bar{r}_o^2}{K}\tau$. The solutions in Fig. 3-7 are for the same conditions as those of Fig. 3-6 except that $S = .1$; but now, as a consequence of assuming S to be constant, the absolute reaction front velocity becomes less than the particle velocity at the front when $\tau \approx 3.3$ for $\bar{r}_o = 6\frac{1}{4}$ microns as shown in Fig. 3-8. The point where $U_p = W_\lambda$ is depicted by the $(+)$ in Figs. 3-7 and 3-8. Although the solution in Fig. 3-7 for $\bar{r}_o = 6\frac{1}{4}$ microns is not physically tenable beyond $\tau \approx 3.3$, the results indicate the influence of S on the transient process. The pressure asymptotes are smaller than in Fig. 3-6, from the results of section 2, but the pressure overshoots are more pronounced than before for corresponding particle sizes. This reflects the fact that the velocity with which the flame overtakes the particles obtains a lower minimum in the transient for $S = .1$ than for $S = .2$ and thus yields a more sudden pressure decrease.

3-2.3. Time Lag Law

Since the particle motion was characterized by a velocity lag relative to the gas phase, the transient process was analyzed for the following particle flow field:

$$U_p(\tau, X) = 0 \qquad , \quad \tau \leq \tau_{lag}$$
$$= U(\tau - \tau_{lag}, X) \qquad , \quad \tau \geq \tau_{lag}$$

so that

$$\frac{y_{px}}{y_{po}} = 1 \qquad , \quad \tau \leq \tau_{lag}$$
$$= P^{1/\gamma}(\tau - \tau_{lag}, X) \qquad , \quad \tau \geq \tau_{lag}$$

where the quantities P and U are functions of τ and X is the unreacted region. To perform the integration, the values for $\frac{y_{px}}{y_{po}}$ and U_{px} must be substituted into Eq. (3-6). Since for each point (τ, X) of the unreacted region there exists a point on the reaction front such that the simple wave emanating from that point passes through (τ, X), these may be expressed in terms of properties at the reaction front at a time τ_x with the aid of the simple wave relations.

The pressure profiles for this case, which are now independent of $\frac{a_{go}\bar{r}_o}{K}$, $\frac{\bar{r}_o}{\lambda}$, and ρ_p, are presented in Fig. 3-9 over a range of τ_{lag} for $\eta_o = .1$ and $S = .2$. By comparison of Figs. 3-6 and 3-9, it is evident that the results for a given set of $\frac{a_{go}\bar{r}_o}{K}$, $\frac{\bar{r}_o}{\lambda}$, and ρ_p can be represented adequately by the solution for a selected τ_{lag}.

3-3. Conclusions

While the propagation velocity in homogeneous flames depends primarily on the state properties and transport coefficients, in

two-phase combustion it depends, in addition, on the relative velocity of the gas and particles. For the flame model assumed here, if the quantity S is too small the particle velocity lag may cause the absolute velocity of the front to become smaller than the local particle velocity during the deceleration period. Consequently, to make the solutions reasonable during the deceleration process, S may have to be chosen so large that, based on experimental and theoretical evidence, it will be unreasonable during the acceleration process. It should be noted that $S = .2$ corresponds to 60 m/sec for this problem (a_o = 330 m/sec; oxygen, 300° K), which is already an order of magnitude higher than the values predicted by Williams [8] based on eigenvalue solutions.

The most significant aspect of this study is the occurrence of the pressure overshoot in the reaction zone, indicating the strong coupling between the thermo-kinetic and gas dynamic processes in two-phase combustion. Since the overshoot is of the same order of magnitude as the asymptotic pressure, and its peak attained in about a millisecond, the results suggest a mechanism for the source of the pressure disturbances in liquid rocket thrust chambers which often amplify to destructive proportions.

4. WAVE POLARS FOR NON-REACTING TWO-PHASE SYSTEMS

In accordance with Idealization 2, heat and mass transfer between phases in the unreacted region were neglected in the analysis of pressure wave generation. The study of the modifications on shock and isentropic processes introduced by the consideration of transport phenomena is therefore of interest. The advent of rocket propulsion technology has already promoted a substantial amount of work in two-phase dynamics [1-7]; however, the problem of shock and rarefaction wave propagation in evaporating two-phase systems has not been treated.

The purpose of this section is to consider the changes of state brought about by the action of shock and rarefaction waves propagating through two-phase mixtures. While the results obtained for the jump conditions across steady-state shock waves are correct regardless of the relaxation phenomena, those for isentropic rarefactions and compressions are essentially approximations since, strictly speaking, the assumption of isentropicity excludes the existence of particle velocity lag throughout the process. The solutions are presented in the form of wave polars similar to those introduced by Oppenheim, Urtiew, and Laderman [26] for the analysis of wave interaction phenomena.

4-1. The Particle-laden Gas

4-1.1. Equilibrium Sound Velocity

The general form of the expression for the equilibrium sound velocity is [27]

$$a_{eq}^2 = \frac{p/\rho}{\frac{\partial \ln \rho}{\partial \ln p} - \frac{p/\rho}{(c_p)_{eq} T}\left(\frac{\partial \ln \rho}{\partial \ln T}\right)^2} \qquad (4\text{-}1)$$

where ρ is the density and $(c_p)_{eq}$ the constant pressure specific heat per unit mass of mixture, and the subscript eq denotes the equilibrium condition. Equation (4-1) and the equation of state enable one to obtain the equilibrium sound velocity.

The equation of state for a gas containing solid particles can be expressed in terms of the volumetric fractions, $\mathcal{V}_i$, and the densities, ρ_i , of the particles and gas, so that

$$\rho = \mathcal{V}_g \rho_g + \mathcal{V}_p \rho_p = \mathcal{V}_g \rho_g (1 + \eta) = \rho_m \qquad (4\text{-}2)$$

where η is the mass loading factor, and the subscripts m , g , and p refer to mixture, gas, and particle quantities respectively. While significant effects of finite particle volume on the dynamics of gas-particle systems were illustrated by Rudinger [7], his results show that the assumption $\mathcal{V}_p \approx 0$ is valid over an important range of application and hence this idealization is invoked here. Consequently, Eq. (4-2), the perfect gas law, and the definition of the mass loading factor yields

$$\rho = \frac{p \mathcal{M}_g}{\mathcal{R} T}(1 + \eta) \qquad (4\text{-}3)$$

where $\mathcal{M}_g$ is the molecular weight of the gas and $\mathcal{R}$ is the universal gas constant.

The specific heat ratio, $\left(\frac{C_p}{C_v}\right)_{eq}$, is obtained from the specific heat equation

$$(C_p)_{eq} - (C_v)_{eq} = \frac{p}{\rho T}\left(\frac{\partial \ln \rho}{\partial \ln T}\right)^2 \Big/ \left(\frac{\partial \ln \rho}{\partial \ln p}\right) \qquad (4\text{-}4)$$

and from Eq. (4-3)

$$(c_p)_{eq} - (c_v)_{eq} = \frac{\mathcal{R}}{\mathcal{M}T} \tag{4-5}$$

Combining Eqs. (4-3) and (4-5) and rearranging yields

$$\left(\frac{c_p}{c_v}\right)_{eq} = \frac{\gamma(1+\delta\eta)}{1+\gamma\delta\eta} \tag{4-6}$$

where γ is the specific heat ratio of the gas phase, and δ is defined by

$$\delta \equiv \frac{(c_p)_p}{(c_p)_g} \tag{4-7}$$

Substituting Eq. (4-3) into Eq. (4-1) gives

$$a_{eq} = \left[\frac{\gamma RT}{m_g}\left(\frac{1+\delta\eta}{1+\gamma\delta\eta}/(1+\eta)\right)\right]^{1/2} \tag{4-8}$$

or

$$\frac{a_{eq}}{a_g} = \left[\frac{1+\delta\eta}{1+\gamma\delta\eta}/(1+\eta)\right]^{1/2} \tag{4-9}$$

Hence the equilibrium sound velocity of the mixture is always less than that of the gas phase, so that the presence of the particles has the effect of slowing down the wave, the same effect as occurs when a gas of higher molecular weight is added to a gas of lower molecular weight. Of course, in this case the heavy gas contributes to the pressure, unlike the particle-laden gas.

4-1.2. The One-dimensional Shock Process

The counterpart of the ideal gas shock relations is obtained for the particle-laden gas from the equation of state, Eq. (4-2), and the well-known Hugoniot equation

$$h_1 - h_0 = \tfrac{1}{2}(p_1 - p_0)(v_1 + v_0) \qquad (4\text{-}10)$$

where h is the enthalpy per unit mass of mixture, v is the mass specific volume of the mixture, and the subscripts 0 and 1 refer to the initial and final states respectively. The non-dimensional form of Eqs. (4-3) and (4-10) are

$$P\bar{V} = \Theta \qquad (4\text{-}11)$$

and

$$\mathcal{H}_1 - \mathcal{H}_0 = \tfrac{1}{2}(P-1)(\bar{V}+1) \qquad (4\text{-}12)$$

in which P is the ratio $\frac{p_1}{p_0}$, $\bar{V} \equiv \frac{v_1}{v_0}$, $\Theta \equiv \frac{T_1}{T_0}$, and $\mathcal{H} \equiv \frac{h}{(pv)_0}$. Eliminating Θ dependence from Eqs. (4-11) and (4-12) gives

$$\bar{V} = \frac{P + \frac{\gamma+1+2\gamma\delta\eta}{\gamma-1}}{\left[\frac{\gamma+1+2\gamma\delta\eta}{\gamma-1}\right]P + 1} \qquad (4\text{-}13)$$

The shock Mach number, M_0, normalized with respect to the gas phase sound velocity in the initial state and obtained from the momentum equation is

$$M_0 = \frac{u_0}{a_{g0}} = \frac{(P-1)/(1-\bar{V})}{\gamma(1+\eta)} \qquad (4\text{-}14)$$

where u_o is the initial velocity relative to the shock wave. Substitution of Eq. (4-13) into Eq. (4-14) leads to

$$M_o = \left[\frac{(\gamma+1+2\gamma\delta\eta)P+\gamma-1}{2\gamma(1+\gamma\delta\eta)(1+\eta)}\right]^{1/2} \tag{4-15}$$

The velocity change across the shock wave, U, is easily seen to be

$$U = M_o(1-V) \tag{4-16}$$

and with Eq. (4-15)

$$U = (P-1)\left[\frac{\frac{2}{\gamma}(1+\gamma\delta\eta)/(1+\eta)}{(\gamma+1+2\gamma\delta\eta)P+\gamma-1}\right]^{1/2} \tag{4-17}$$

If the shock velocity is supersonic, $M_o > 1$, the shock will consist of a shock front followed by a relaxation zone. However, when P satisfies

$$1 \leq P \leq \frac{\gamma+1+2\gamma\delta\eta+2\gamma^2\delta\eta(1+\eta)}{\gamma+1+2\gamma\delta\eta} \tag{4-18}$$

and hence the values of M_o are

$$\frac{(1+\delta\eta)/(1+\eta)}{1+\gamma\delta\eta} < M_o \leq 1 \tag{4-19}$$

the shock velocity is less than the gas sonic velocity in the undisturbed region. As a result of $M_o < 1$, the shock wave will be fully diffused and the gas and particle properties will vary continuously through the shock wave. Similar phenomena occur in reacting gas flows [6].

The Mach number, $\bar{M}$, and velocity change, $\bar{U}$, normalized with respect to the equilibrium sound velocity of the initial mixture are obtained by dividing Eqs. (4-15) and (4-17) by Eq. (4-9):

$$\bar{M}_o = \left[\frac{(\gamma+1+2\gamma\delta\eta)P+(\gamma-1)}{2\gamma(1+\delta\eta)}\right]^{1/2} \tag{4-20}$$

$$\bar{U} = (P-1)(1+\gamma\delta\eta)\left[\frac{\frac{2}{\gamma}/(1+\delta\eta)}{(\gamma+1+2\gamma\delta\eta)P+\gamma-1}\right]^{1/2} \tag{4-21}$$

Hence, as $P \to 1$, $\bar{M}_o \to 1$, so that the wave velocity for vanishingly small pressure ratios is the equilibrium sound velocity.

4-1.3. The One-dimensional Isentropic Process

The particle-laden gas isentropic relations are obtained with the aid of the equation of state, Eq. (4-2), and the isentropic condition

$$(c_p)_{eq}\, dT = -\frac{1}{\rho}\left(\frac{\partial \ln \rho}{\partial \ln T}\right) dp \tag{4-22}$$

Combining these with the aid of the definitions of δ, η, γ, and the non-dimensional variables, there results in integrated form:

$$\Theta = P^{\frac{\gamma-1}{\gamma}/(1+\delta\eta)} \tag{4-23}$$

and hence

$$\bar{V} = P^{-\frac{1}{\gamma}\left[\frac{1+\gamma\delta\eta}{1+\delta\eta}\right]} \tag{4-24}$$

The change in particle velocity across the isentropic expansion or compression is given by the invariant relation

$$u - u_o = \int_{\rho_o}^{\rho} a_{eq} \frac{d\rho}{\rho} \tag{4-25}$$

and with the help of Eqs. (4-22) and (4-23),

$$U = \frac{2}{\gamma - 1}\left[\frac{1+\gamma\delta\eta}{1+\eta}(1+\delta\eta)\right]^{1/2}\left[P^{\frac{\gamma-1}{2\gamma}/(1+\delta\eta)} - 1\right] \tag{4-26}$$

4-2. The Gas-Liquid-Vapor System

The system consists of an ideal gas component with constant specific heat and a condensed component with a finite vapor pressure. It is assumed that the vapor behaves as an ideal gas and that both phases of this component have constant specific heats. The volumetric fraction of the condensed phase is again considered to be negligible.

4-2.1. Equilibrium Thermodynamics

The equilibrium composition of this system is determined by the thermodynamics of the condensed component in terms of the independent variables, p and T. Since for equilibrium the Gibbs free energy, g, of the two phases must be equal,

$$g_c^*(T) + \int_{p_o}^{p} v_c \, dp = g_v^*(T) + \int_{p_o}^{p} v_v \, dp \tag{4-27}$$

where subscripts c and v denote the condensed and vapor phase, and the superscript $*$ refers to quantities at the initial

pressure, p_o. Since $v_c \sim o$, and the vapor obeys the ideal gas law, Eq. (4-26) becomes

$$g_c^*(T) = g_v^*(T) + \frac{RT}{m_v} \log\left[\frac{(pz_v)}{(pz_v)_o}\right] \qquad (4\text{-}28)$$

where z is the mole fraction based on one mole of gas component plus vapor and m_v is the molecular weight of the component in condensed phase. Hence,

$$z_v = \frac{(pz)_o}{p} \exp\left[\frac{g_c^* - g_v^*}{RT/m_v}\right] \qquad (4\text{-}29)$$

The quantity $\frac{g_c^* - g_v^*}{RT/m_v}$, a function of the temperature alone, can be expressed in terms of its value at the initial temperature, the constant properties of the component, P, and Θ, so that

$$z_v = \frac{z_{vo}}{P} \exp\left[\frac{\gamma_o \sigma}{\gamma - 1}(\delta_c - \delta_v)\left(1 - \frac{1}{\Theta} - \ln\Theta\right) + H_v\left(1 - \frac{1}{\Theta}\right)\right] \qquad (4\text{-}30)$$

where σ is the molecular weight ratio of condensed to gaseous component, δ is the constant pressure mass specific heat of the condensed component divided by that of the gaseous component, and H_v is the non-dimensional heat of evaporation at the initial state, $H_v \equiv \left(\frac{h_v - h_c}{RT/m_v}\right)_o$.

The initial ratio of mass in the condensed phase to that in the gas-vapor material is

$$\eta = \left(\frac{z_c \sigma}{z_v \sigma + z_g}\right)_o = \left(\frac{z_c \sigma}{z_v \sigma + (1 - z_v)}\right)_o \qquad (4\text{-}31)$$

while the mass of the component in the condensed phase divided by the gas component mass, an invariant, is

$$\eta' = \frac{(Z_v + Z_c)\sigma}{1 - Z_v}$$

or

$$Z_c = \frac{\eta'}{\sigma} - Z_v\left(1 + \frac{\eta'}{\sigma}\right) \qquad (4\text{-}32)$$

It is not possible to determine a priori whether or not Z_c will be positive from Eq. (4-31), but rather it must be found a posteriori. In the event Eq. (4-31) yields a negative quantity, Z_c is to be set equal to zero and

$$Z_v = \frac{\eta'/\sigma}{1 + \eta'/\sigma} \qquad (4\text{-}33)$$

The molecular weight of the mixture, $\mathcal{M}_m$, also an invariant, is

$$\mathcal{M}_m = \mathcal{M}_g(1 + \eta')/(1 + \eta'/\sigma) \qquad (4\text{-}34)$$

where $\mathcal{M}_g$ is the molecular weight of the gaseous component. The equation of state, given by Eq. (4-2), is most conveniently expressed as

$$V = \frac{RT}{P\mathcal{M}_m}/(1 + Z_c) \qquad (4\text{-}35)$$

or in terms of non-dimensional variables

$$\overline{V} = \frac{\Theta}{P}\frac{(1+Z_c)_o}{(1+Z_c)} \qquad (4\text{-}36)$$

Differentiating Eq. (4-30), there results

$$\left.\begin{aligned} \frac{\partial \ln Z_v}{\partial \ln \theta} &= \frac{\gamma\sigma}{\gamma-1}(\delta_c-\delta_v)\left(\frac{1}{\theta}-1\right)+H_v/\theta \\ \frac{\partial \ln Z_v}{\partial \ln P} &= -1 \end{aligned}\right\} Z_c>0 \qquad (4\text{-}37)$$

$$\frac{\partial \ln Z_v}{\partial \ln \theta} = \frac{\partial \ln Z_v}{\partial \ln P} = 0 \quad , \quad Z_c = 0$$

and from Eqs. (4-30) and (4-34),

$$\left.\begin{aligned} \frac{\partial \ln \bar{V}}{\partial \ln \theta} &= 1+\frac{Z_v}{1-Z_v}\frac{\partial \ln Z_v}{\partial \ln \theta} \\ \frac{\partial \ln \bar{V}}{\partial \ln P} &= -1+\frac{Z_v}{1-Z_v}\frac{\partial \ln Z_v}{\partial \ln P} \end{aligned}\right\} \qquad (4\text{-}38)$$

The non-dimensional enthalpy is

$$\mathcal{H} \equiv \frac{h}{(pv)_o} = \left\{\frac{\gamma}{\gamma-1}\left[(1-Z_v)+\sigma(\delta_v Z_v+\delta_c Z_c)\right](\theta-1)-Z_c H_v\right\}\frac{(1+Z_v)_o}{(1+Z_v)} \qquad (4\text{-}39)$$

and the non-dimensional frozen specific heat is

$$(\bar{C}_p)_{fz} \equiv \frac{(c_p)_{eq}}{(pv/T)_o} = \frac{\gamma}{\gamma-1}\left[(1-Z_v)+\sigma(\delta_v Z_v+\delta_c Z_c)\right]\frac{(1+Z_v)_o}{(1+Z_v)} \qquad (4\text{-}40)$$

while the non-dimensional equilibrium specific heat is

$$(\bar{C}_p)_{eq} = (\bar{C}_p)_{fz}+\frac{1}{\theta}\left[\frac{\gamma\sigma}{\gamma-1}(\delta_v-\delta_c)(\theta-1)+H_v\right]\frac{Z_v}{1-Z_v}\frac{(1+Z_v)_o}{(1+Z_v)}\frac{\partial \ln Z_v}{\partial \ln \theta} \qquad (4\text{-}41)$$

It is interesting to note that since the derivatives of the mole fractions defined by Eq. (4-37) are discontinuous at points where Z_c becomes zero, the derivatives of $\bar{V}$ and $\mathcal{H}$, defined by Eqs. (4-36) and (4-41), respectively, are also discontinuous there.

The thermodynamic state of the system is now determined in terms of the independent variables P and Θ, and the six parameters, δ_c, δ_v, η, Z_{vc}, H_v and σ.

4-2.2. The One-dimensional Shock Process

The thermodynamic state data, the Hugoniot equation, Eq. (4-11), together with a value of the shock strength parameter, the pressure ratio, P, determine conditions at the end points of the wave. However, it is not possible to obtain explicit solutions for these equations and consequently they have been solved numerically with the aid of the Newton-Raphson technique on an IBM 1620 digital computer. Once the state properties on the Hugoniot curve are determined for a given value of the pressure ratio, P, the shock Mach number and velocity change across the wave may be determined similarly to Eqs. (4-14) and (4-16). It should be noted that the solutions obtained here are independent of the initial state.

4-3. Results

4-3.1. The Particle-laden Gas

Figure 4-1 shows the influence of η and δ on the $P-U$ shock polar for the particle-laden gas for $\gamma=1.4$. The polars are substantially modified by the loading factor η, while the ratio of heat capacities, δ, is of secondary importance. In the

plane solution displayed in Fig. 4-2, however, where $A = \theta^{1/2}$, the influence of both δ and η is significant. Consequently, wave interaction processes will be substantially modified by δ due to its influence on the sound velocity behind the wave. The effects of η and δ on rarefactions are similar to those on shock waves as shown in Figs. 4-3 and 4-4. The purpose of the "windows" in Figs. 4-1 and 4-3 is to permit the construction of the polars for any given η and δ where $0 \leq \eta \leq 2$ and $0 \leq \delta \leq 2$.

Figure 4-5 is a schematic representation of a problem worked out by Rudinger and Chang [5] which involved the formation of a shock wave in a gas-particle mixture by an impulsively accelerated piston. The values of γ, η, and δ for their problem were .3, 1.125, and 1.4, respectively, and the problem was determined by setting the initial Mach number to 1.30. With the aid of the shock polars, the end points of this problem can be found immediately as shown in Fig. 4-6. The P-U polars and P-M curves for the ideal gas phase and for the mixture are given in Fig. 4-6, and conditions at ①, ②, and ③ refer to the state properties of the gas at time zero, of the relaxed mixture at the steady state, and of the gas behind the shock front at the steady state, respectively. Points on line ① in Fig. 4-6 are determined by the data, $M_1 = 1.3$, which in turn gives the piston velocity, U_{PISTON}, since the gas and piston must initially move together. Line ② is then fixed by U_{PISTON} and knowing the value of the steady-state Mach number, M_{SHOCK}, the conditions behind the steady-state gas shock, line ③, can be determined. The numbers included in Fig. 4-6 are those reported by Rudinger and Chang [5]

and agree within graphical error of the polar solutions. Once the pressures at the different points are known, the A-U polars will give the corresponding temperatures and densities.

Several interesting points may be deduced from Fig. 4-6.

(1) The gas velocity behind the shock decreases from .44 at time zero to .20 at the steady state and the shock Mach number decreases from 1.30 to 1.12, which gives the shock front the curvature displayed in Fig. 4-6. Consequently, both the particles and the gas will be accelerated in the relaxation zone, even at the steady state.

(2) The steady-state velocity of the gas behind the shock front and relative to the wave is $M_{SHOCK} - U_{SHOCKED\ GAS} = .92$, while the velocity of the relaxed mixture relative to the wave is $M_{SHOCK} - U_{PISTON} = .68$. Hence, both the particles and the gas decelerate relative to the steady-state wave in the relaxation zone.

(3) The pressure increases through the relaxation zone.

Note that if $M_{SHOCK} < 1$, it is not possible for a discontinuous shock front to exist so the gas and particle velocity will vary continuously through the wave.

Whereas M_1 was used to determine the problem here, the polars permit several possible points of departure for solving the problem, such as U_{PISTON}, M_{SHOCK}, P_1, P_2, etc.

4-3.2. The Gas-Liquid-Vapor System

The solutions of the gas-liquid-vapor systems showed that the Mach number and velocity change across a shock wave were affected very little by the occurrence of evaporation if the

Table 4-1. Velocity Change, $\tilde{U}$, for $P=10$ and $\eta=1$. The gas-particle solutions for a δ of 1 and 2 are 1.93 and 1.96 respectively.

			$(Z_v)_0=0.015$		$(Z_v)_0=0.500$	
H_v	δ_v	σ	$\delta_c/\delta_v=1$	$\delta_c/\delta_v=2$	$\delta_c/\delta_v=1$	$\delta_c/\delta_v=2$
10	1	1	1.93	1.96	1.93	1.95
		2	1.93	1.96	1.95	1.98
	2	1	1.96	1.98	1.96	2.00
		2	1.96	1.98	1.98	2.03
20	1	1	1.96	1.97	1.97	1.97
		2	1.96	1.96	1.97	1.99
	2	1	1.97	1.98	1.98	1.98
		2	1.97	1.98	1.98	1.99

Table 4-2. Mach Number, $\tilde{M}$, for $P=10$ and $\gamma=1$. The gas-particle solutions for a δ of 1 and 2 are 2.34 and 2.30 respectively.

			$(Z_v)_0=0.015$		$(Z_v)_0=0.500$	
H_v	δ_v	σ	$\delta_c/\delta_v=1$	$\delta_c/\delta_v=2$	$\delta_c/\delta_v=1$	$\delta_c/\delta_v=2$
10	1	1	2.34	2.30	2.34	2.32
		2	2.34	2.30	2.31	2.28
	2	1	2.30	2.27	2.30	2.26
		2	2.30	2.28	2.26	2.22
20	1	1	2.30	2.29	2.29	2.28
		2	2.30	2.29	2.28	2.28
	2	1	2.30	2.27	2.28	2.28
		2	2.29	2.28	2.27	2.26

Table 4-3. Sound Velocity of Gas Phase, $A = \frac{a_g}{a_{go}}$, for $P = 10$ and $\eta = 1$. The gas-particle solutions for a δ of 1 and 2 are 1.32 and 1.22 respectively.

			$(Z_v)_0 = 0.015$		$(Z_v)_0 = 0.500$	
H_v	δ_v	σ	$\delta_c/\delta_v = 1$	$\delta_c/\delta_v = 2$	$\delta_c/\delta_v = 1$	$\delta_c/\delta_v = 2$
10	1	1	1.29	1.22	1.15	1.16
		2	1.23	1.21	1.12	1.17
	2	1	1.21	1.14	1.14	1.15
		2	1.19	1.14	1.15	1.25
20	1	1	1.14	1.13	1.07	1.07
		2	1.05	1.07	1.04	1.04
	2	1	1.11	1.10	1.06	1.06
		2	1.04	1.07	1.04	1.06

correct specific heat ratio of the gas and vapor is accounted for in non-dimensionalizing the velocities, although the temperatures, densities, and mass loading factor were substantially changed. Hence, the solutions for $\tilde{U}$ and $\tilde{M}$ defined by

$$\tilde{U} \equiv \frac{u}{(PV_g)_o} \quad , \qquad \tilde{M} \equiv \frac{u_o}{(PV_g)_o}$$

are given in Tables 4-1 and 4-2 respectively for the specific heat ratio of the gas component equal to 1.4, $\gamma = 1.$, and $P = 10$ for two representative values each of δ_v, δ_c, H_v, Z_{vo}, and σ. The difference in values between $\tilde{U}$ and $\tilde{M}$ in Tables 4-1 and 4-2 and those for the gas-particle system are less than 0.06 and 0.07 respectively.

Table 4-3 gives the values of $A = \frac{a_g}{a_{go}}$ for the same conditions as in Tables 4-1 and 4-2 and indicates the significant influence of evaporation on the solution for A. Hence the effect of evaporation is an important consideration in the analysis of wave interaction problems.

From Tables 4-1 and 4-2, it can be concluded that the influence of evaporation on the solution to the problem of Rudinger and Chang [5], Fig. 4-6, is negligible if $\tilde{U}$ and $\tilde{M}$ are used in place of U and M. For example, U_{PISTON} is .442 in Fig. 4-6 whence $\tilde{U}_{PISTON}$ is .526, and, for the extreme case in Table 4-1, for the case with evaporation is the same as that shown in Fig. 4-6 to at least two decimal places.

4-4. Conclusions

The relationship between the pressure and the velocity change across wave processes is essentially dependent on the

mass loading ratio of the initial mixture, as well as the Mach number, independently of the occurrence of evaporation and heat transfer to the condensed phase of the mixture.

However, the temperature and density behind the wave are dependent on these processes. This implies, then, that the development of heterogeneous combustion will be affected by these phenomena, since it depends on the density of the oxidizer and fuel vapor that crosses the reaction front. In cases where the vapor pressure is low, however, the process will still be essentially independent of evaporation.

5. CONCLUDING REMARKS

The generation of the flow field in a particle-fueled combustion system is accompanied by:

(1) rapid development of large pressures which are strongly dependent upon the loading factor, flame speed, and particle motion, and

(2) significant overshoots relative to the final steady state which occur in the transient process.

Both of these points demonstrate the importance of the link between chemico-kinetic and gas-dynamic processes in two-phase combustion. Several facets of the problem which should be studied in order to understand more fully and control the process are here discussed.

(a) Mass Generation

Consideration of the fuel vapor in the unreacted region has been neglected in the analysis of pressure wave generation. This is a good approximation for fuels with a low vapor pressure, such as hydrazine, and the transport phenomena will not influence the process significantly. However, for fuels with a high vapor pressure, evaporation in the compression region will be important since then the vapor will react immediately upon entering the reaction zone, which will severely modify the transient development as well as the steady-state solution.

The mass generation law used in this study, Eq. (2-30), has been found to be quite valid for the burning of single drops

in a stagnant atmosphere [23]. In this problem, however, there is a gas velocity relative to the particles, and the state properties of the ambient atmosphere change significantly. Hence the effect of a more sophisticated mass release rate in the reaction zone should be investigated, so that its dependence on the vapor pressure, drop size, the pressure and temperature of the gas, and the various non-dimensional parameters which characterize the problem would be taken into account.

(b) Particle Size Distribution

The particles were characterized by a single size in the analysis. Consequently, all particles were accelerated uniformly in the compression region and reacted uniformly in the reaction zone. If there is a size distribution, a separation will occur in the compression fan according to particle size, since small particles are accelerated more readily than large ones. In addition, the mass release rate will be modified due to the size distribution.

(c) Particle Shattering

It is well known [18, 28] that particle shattering (and/or "exploding") drastically modifies gas-particle dynamics so that this will in turn have a profound influence on the development process.

(d) Flame Model

A constant pressure flame which propagates with a constant velocity relative to the gas phase was assumed in the analysis.

The more "explosive" flames will be accompanied by a significant pressure drop, however, so that even higher pressures will be obtained ahead of the reaction front. This, together with the mechanics of non-steady two-phase flame propagation, should be accounted for in the analysis.

(e) The Chemical System

Hydrazine was used in the analysis because of its low vapor pressure and representative energy of combustion. Different fuels should be analyzed to determine the effect of heating values, equilibrium chemistry, and mole number amplification. More important, it may be possible to alter the combustion kinetics and particle shattering by chemical additives, and hence lead to a more controllable process.

(f) Characteristic Analysis

Once the important features of non-steady two-phase combustion are properly understood by means of the studies outlined above, the problem should be treated more in detail by the use of the method of characteristics. The differences will perhaps be most pronounced in the pressure overshoot phenomena since the properties in the reaction will no longer be constrained to spatial uniformity, but rather they will be permitted to vary in the reaction zone, yielding more "freedom" to the overshoot.

(g) Multidimensional Effects

The transient acceleration process in the analysis that has been presented is due entirely to the extended reaction zone

of the particle flame. In homogeneous flames, however, the flame acceleration is caused predominantly by the growth of the combustion front which results in the increase of the rate of energy release. Hence these effects should be investigated in heterogeneous combustion, and compared with the influence of the extended reaction zone on the flame acceleration.

(h) Wave Interaction Processes

A thorough understanding of the effects resulting from the interaction of flames and pressure waves in non-steady two-phase media is important for deciphering combustion phenomena in liquid rocket thrust chambers. With the aid of the work outlined above, a variety of these interaction problems can now be attacked from a very basic standpoint, which should lead to a more complete grasp of the principles involved.

REFERENCES

1. Marble, F. E., "Dynamics of a Gas Containing Small Solid Particles," Fifth AGARD Colloquium (Pergamon Press, London), 1963, pp. 175-215.
2. Soo, S. K., "Gas Dynamic Processes Involving Suspended Solids," A.I.Ch.E.J., 7: 384-391, 1961.
3. Kriebel, A. R., "Analysis of Normal Shock Waves in Particle Laden Gas," ASME Trans., Series D., J. of Basic Eng., 86: 655-665, 1964.
4. Rudinger, G., "Some Properties of Shock Relaxation in Gas Flows Carrying Small Particles," Phys. of Fluids, 7: 658-663, 1964.
5. Rudinger, G., and Chang, A., "Analysis of Nonsteady Two-Phase Flow," Phys. of Fluids, 7: 1747-1754, 1964.
6. Kliegel, J. R., "Gas Particle Nozzle Flows," Ninth Symposium (International) on Combustion (Academic Press, Inc., New York), 1963, pp. 811-826.
7. Rudinger, G., "Dynamics of Gas-Particle Mixtures with Finite Particle Volume," A.I.A.A. Paper No. 65-9, presented at A.I.A.A. 2nd Aerospace Sciences Meeting, New York, 1965.
8. Williams, F. A., "Monodisperse Spray Deflagration," Liquid Rockets and Propellants, Vol. 2 of Progress in Astronautics and Rocketry (Academic Press, New York), 1960, pp. 229-264.
9. Williams, F. A., "Detonations in Dilute Sprays," Detonation and Two-Phase Flow, Vol. 6 of Progress in

Astronautics and Rocketry (Academic Press, New York), 1962, pp. 99-114.

10. Williams, F. A., Combustion Theory (Addison-Wesley Publishing Company, Inc., Reading, Mass.), 1965, esp. Chapter 11, "Spray Combustion," pp. 250-287.

11. Crocco, L., Grey, J., and Harrje, D. T., "On the Importance of the Sensitive Time Lag in Longitudinal High Frequency Rocket Combustion Instability," Jet Propulsion, 28: 841-843, 1958.

12. Crocco, L., Grey, J., and Harrje, D. T., "Theory of Liquid Propellant Rocket Combustion Instability and its Experimental Verification," A.R.S.J. 30, 159-168, 1960.

13. Crocco, L., Harrje, D. T., Reardon, F. H., "Transverse Combustion Instability in Liquid Propellant Rocket Motors," A.R.S.J., 32: 366, 1962.

14. Crocco, L., "Theoretical Studies on Liquid Propellant Rocket Instability," Tenth Symposium (International) on Combustion, August 17-21, 1964, Cambridge, England (in press).

15. Sirignano, W. A., and Crocco, L., "A Shock Wave Model of Unstable Rocket Combustors," A.I.A.A.J., 2(7): 1285-1296, 1964.

16. Strahle, W. C., "Periodic Solutions to a Convective Droplet Burning Problem: The Stagnation Point," Tenth Symposium (International) on Combustion, August 17-21, 1964, Cambridge, England (in press).

17. Chinitz, W., and Agosta, V. D., "Shock Wave Propagation in Liquid Propellant Rocket Engines," Pyrodynamics, 1(4): 299-317, 1964.

18. Burstein, S. F., Hammer, S. S., Agosta, V. D., "Spray Combustion Model with Droplet Breakup: Analytical and Experimental Results," Detonation and Two Phase Flow, Vol. 6 of Progress in Astronautics and Rocketry (Academic Press, New York), 1962, pp. 243-267.

19. Laderman, A. J., and Oppenheim, A. K., "Initial Flame Acceleration in an Explosive Gas," Proc. Roy. Soc. (London), A268: 153-180, 1962.

20. Laderman, A. J., Urtiew, P. A., and Oppenheim, A. K., "On the Generation of a Shock Wave by Flame in an Explosive Gas," Ninth Symposium (International) on Combustion (Pergamon Press, New York and London), 1963, pp. 265-274.

21. Urtiew, P. A., Laderman, A. J., and Oppenheim, A. K., "Dynamics of the Generation of Pressure Waves by Accelerating Flames," Tenth Symposium (International) on Combustion, August 17-21, 1964, Cambridge, England (in press).

22. JANAF Thermochemical Data, compiled by the Dow Chemical Company, Midland, Michigan, 1964.

23. Godsave, G. A. E., "Studies of the Combustion of Drops in a Fuel Spray--the Burning of Single Drops of Fuel," Fourth Symposium (International) on Combustion (Williams and Wilkins Company, Baltimore), 1953, pp. 818-830.

24. Gilbert, M., Davis, L., and Altman, D., "Velocity Lag of Particles in Linearly Accelerated Combustion Gases," A.R.S.J., 25: 25-30, 1955.

25. Courant, R., and Friedrichs, K. O., Supersonic Flow and Shock Waves (Interscience Publishers, Inc., New York), 1948.

26. Oppenheim, A. K., Urtiew, P. A., and Laderman, A. J., "Vector Polar Method for the Evaluation of Wave Interaction Processes," The Archives of Mechanical Engineering, Polish Academy of Sciences, 11(3): 441-495, 1964.

27. Busch, C. W., Laderman, A. J., and Oppenheim, A. K., "Computation of Gaseous Detonation Parameters," SSL Tech. Rept. #6, and IER Rept. 64-12, University of California, August, 1964.

28. Levine, R. S., "Experimental Status of High Frequency Liquid Rocket Combustion Instability," Tenth Symposium (International) on Combustion, August 17-21, 1964, Cambridge, England (in press).

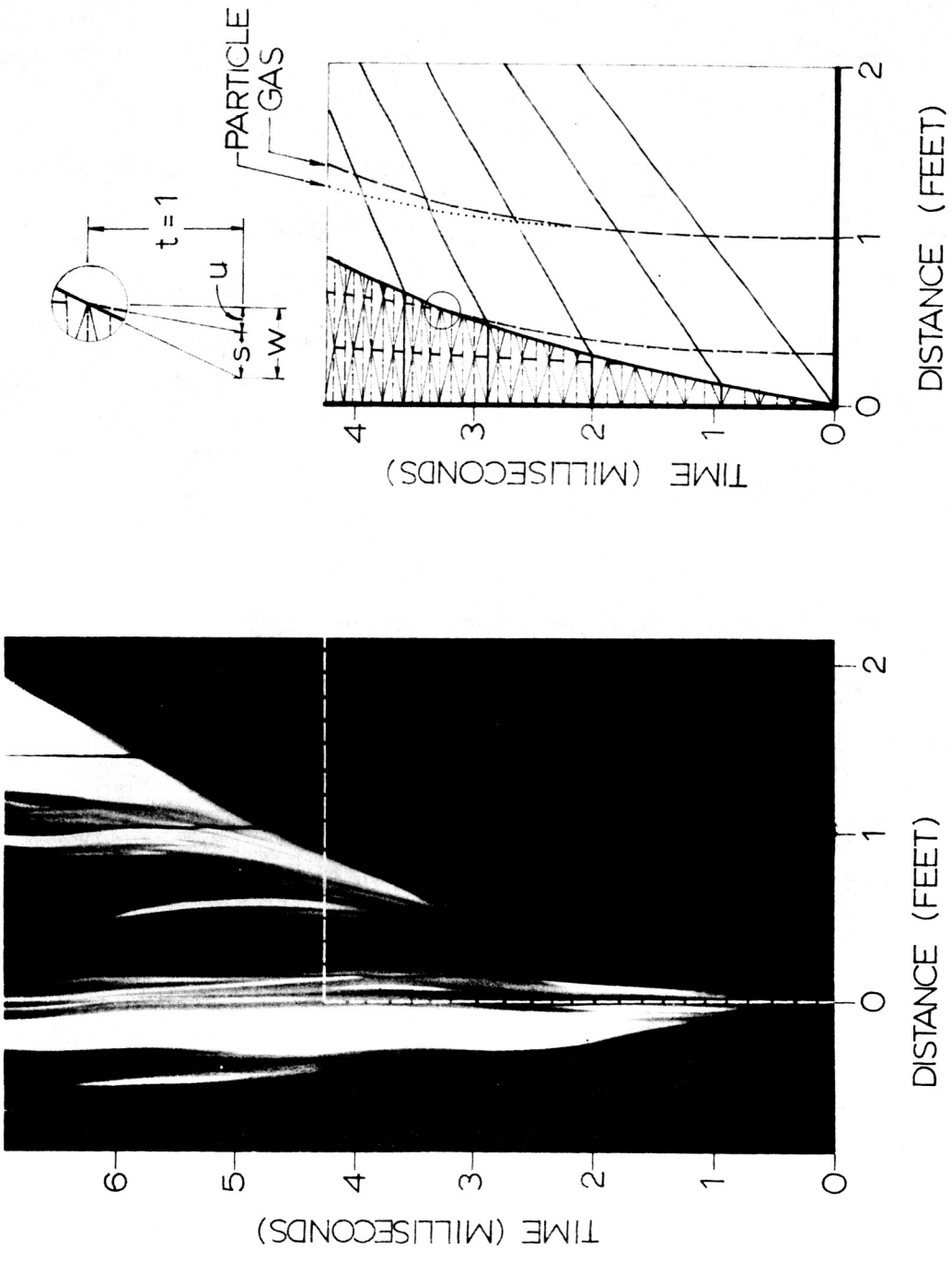
PARTICLE
GAS
t = 1
u
s+t
W
TIME (MILLISECONDS)
DISTANCE (FEET)
0
1
2
3
4
5
6

FIG 1-1

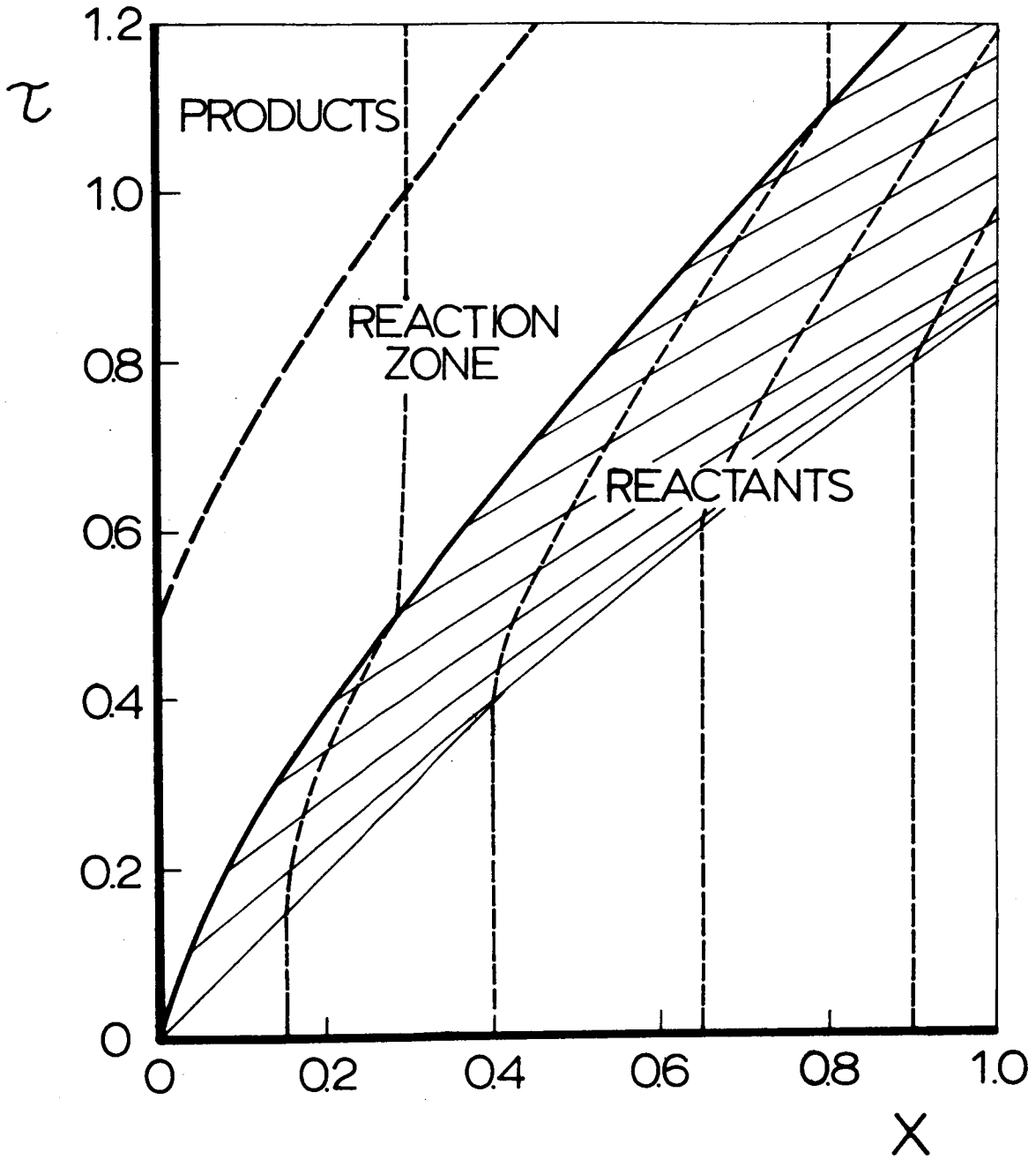
τ
1.2
1.0
0.8
0.6
0.4
0.2
0
PRODUCTS
REACTION ZONE
REACTANTS
0
0.2
0.4
0.6
0.8
1.0
X

FIG. 2-1

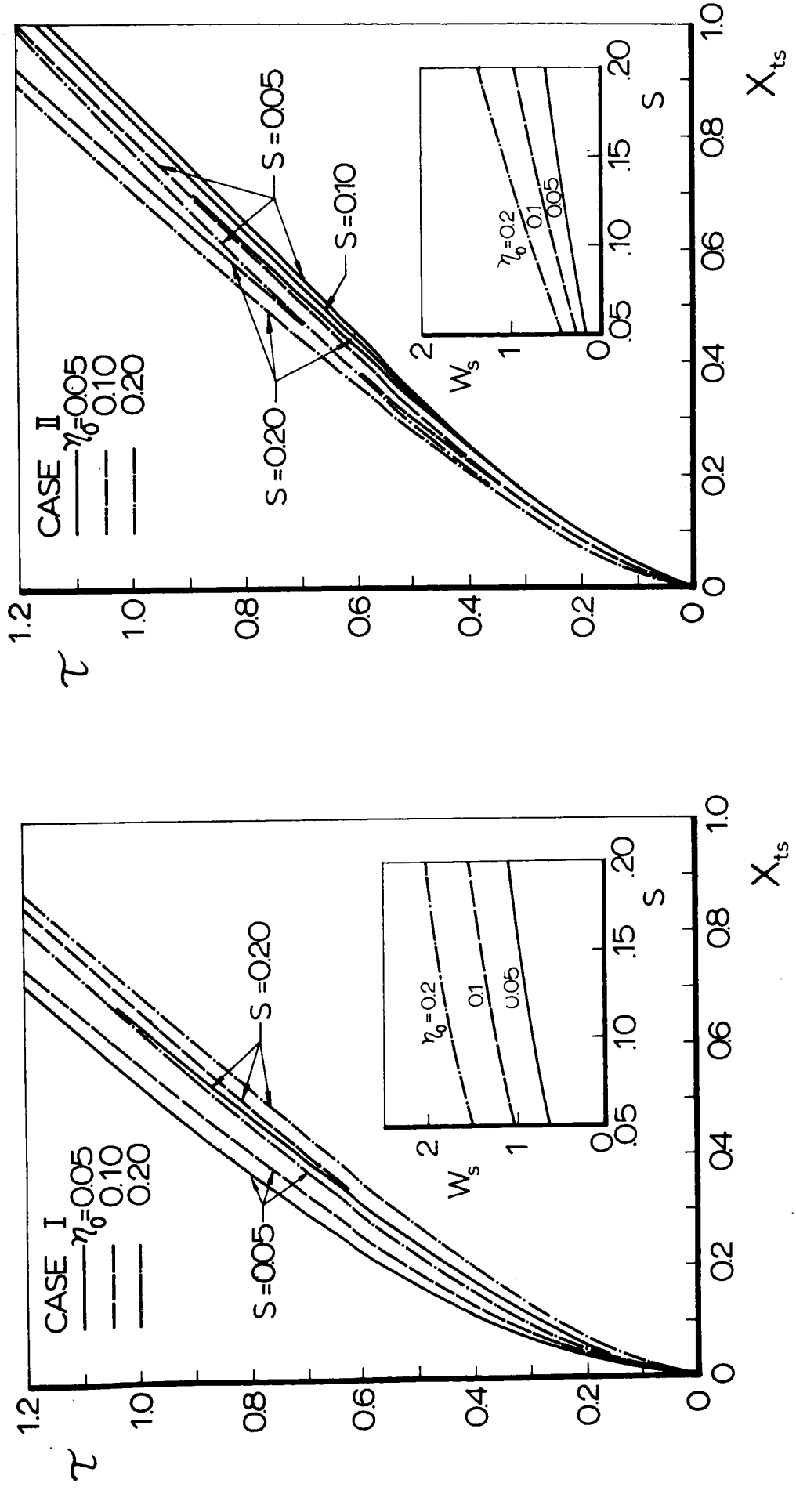
CASE I
η_0=0.05
0.10
0.20
S=0.20
S=0.05
W_s
η_0=0.2
0.1
0.05
S
τ
X_{ts}
CASE II
η_0=0.05
0.10
0.20
S=0.05
S=0.10
S=0.20
W_s
η_0=0.2
0.1
0.05
S
τ
X_{ts}

FIG. 2-2

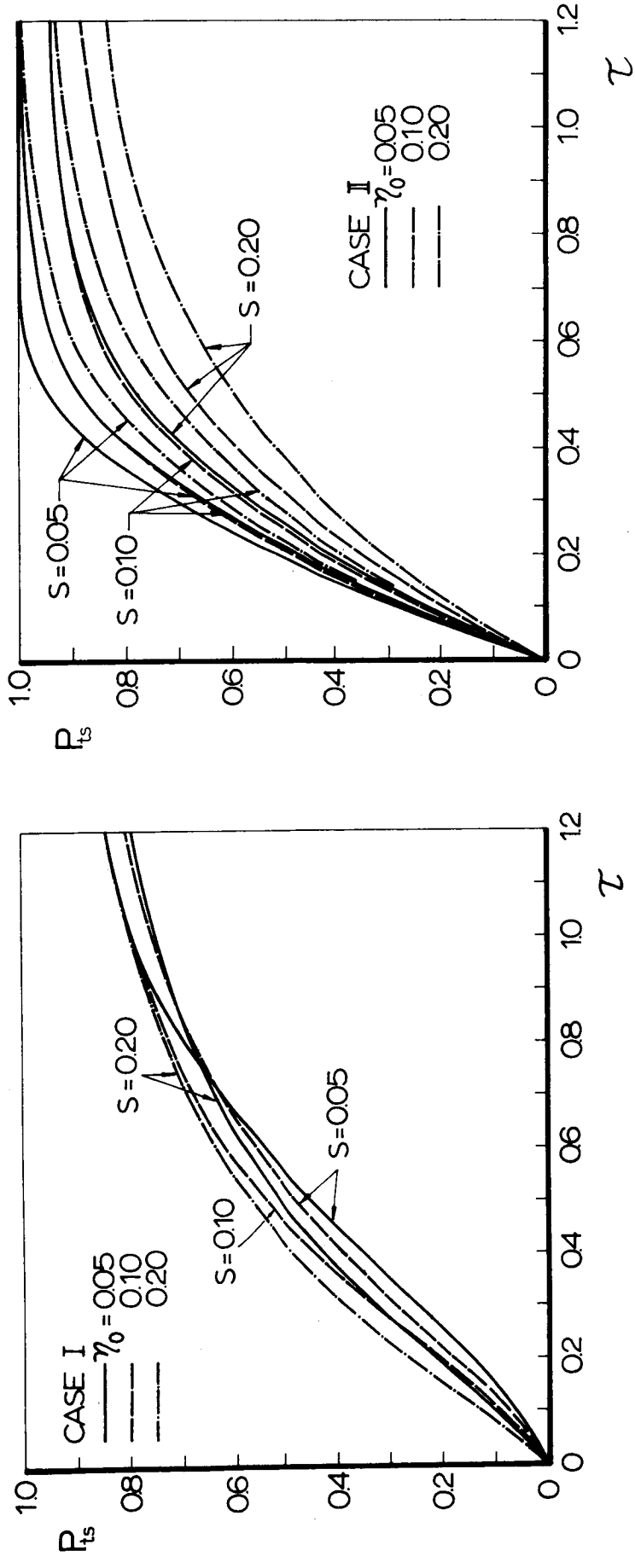
CASE I
η_0 = 0.05
0.10
0.20
S=0.20
S=0.10
S=0.005
P_{ts}
τ
CASE II
η_0=0.05
0.10
0.20
S=0.05
S=0.10
S=0.20
P_{ts}
τ

FIG. 2-3

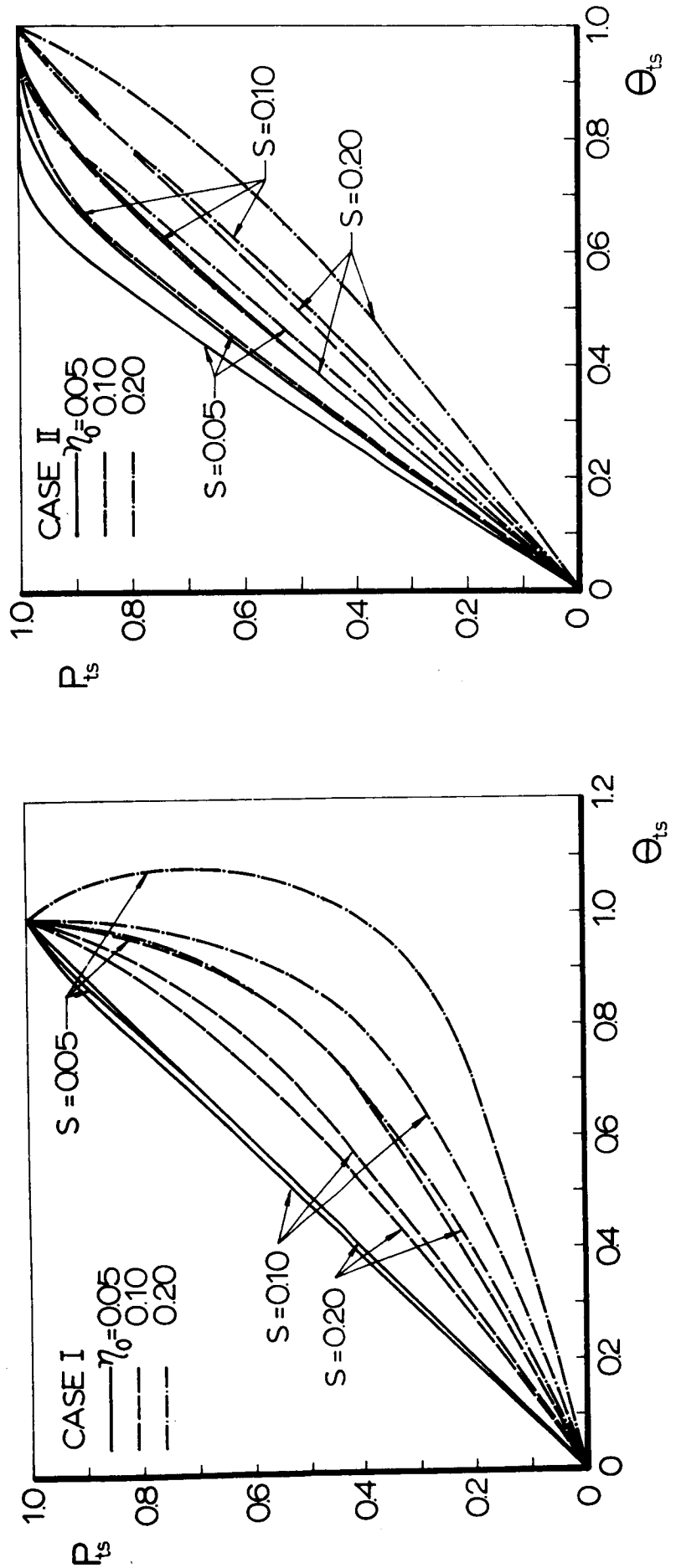
CASE II
η_0=0.05
0.10
0.20
S=0.05
S=0.10
S=0.20
P_{ts}
θ_{ts}
0
0.2
0.4
0.6
0.8
1.0
CASE I
η_0=0.05
0.10
0.20
S=0.05
S=0.10
S=0.20
P_{ts}
θ_{ts}
0
0.2
0.4
0.6
0.8
1.0
1.2

FIG. 2-4

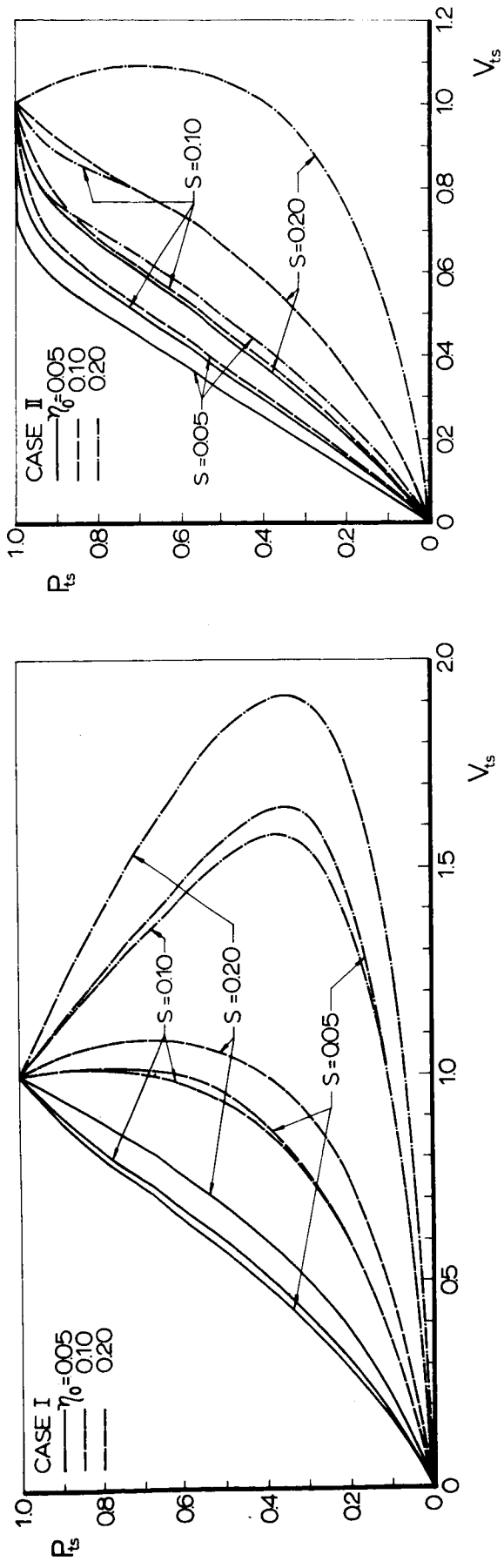
CASE II
η_0=0.05
0.10
0.20
S=0.005
S=0.10
S=0.20
P_{ts}
V_{ts}
CASE I
η_0=0.05
0.10
0.20
S=0.10
S=0.20
S=0.005
P_{ts}
V_{ts}

FIG. 2-5

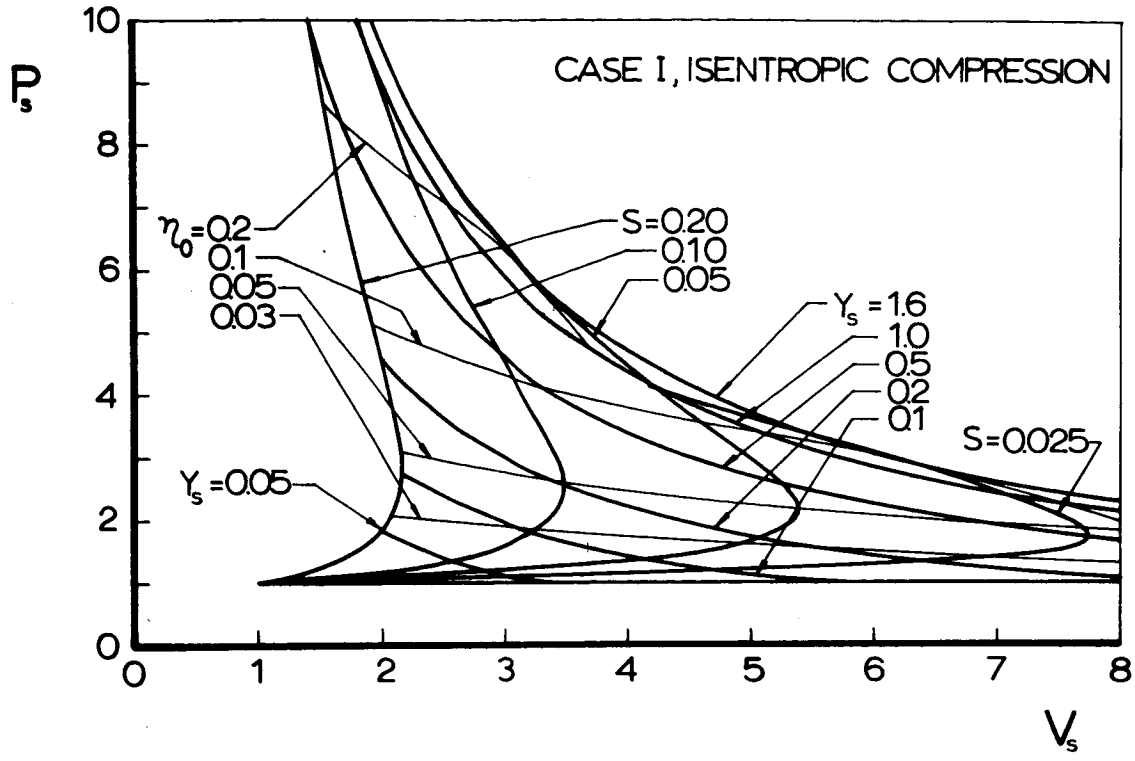
CASE I, ISENTROPIC COMPRESSION
P_s
V_s
η_0=0.2
0.1
0.05
0.03
Y_s=0.05
S=0.20
0.10
0.05
Y_s=1.6
1.0
0.5
0.2
0.1
S=0.025

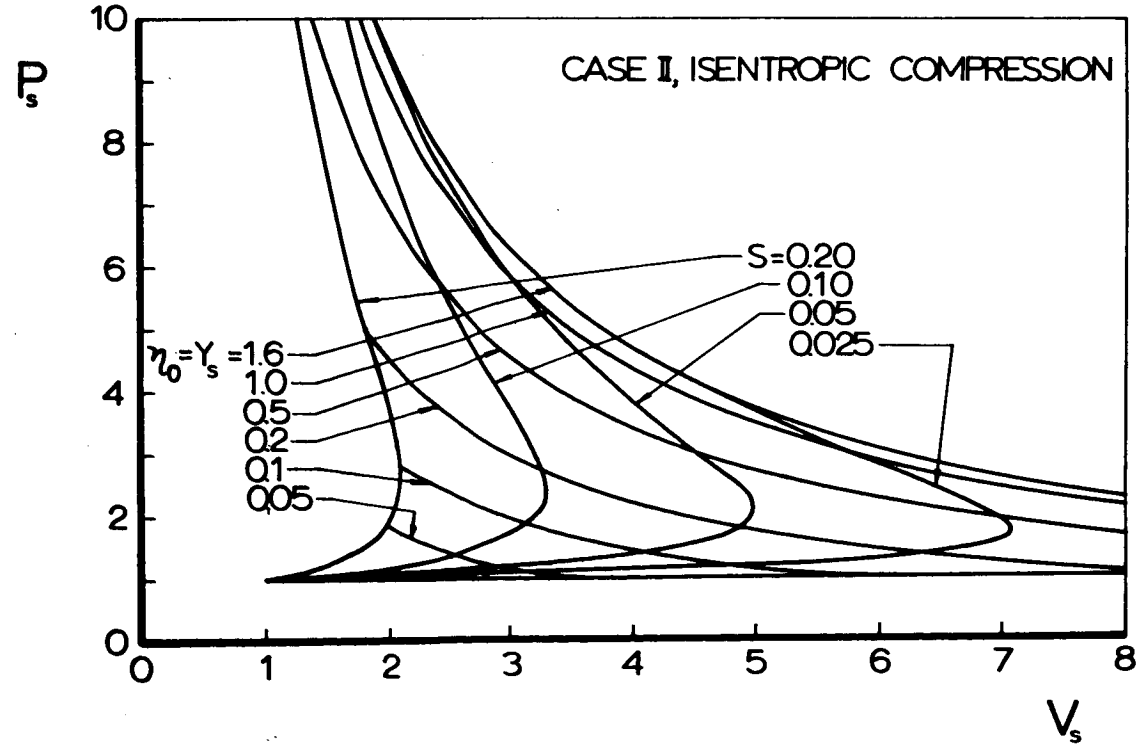
CASE II, ISENTROPIC COMPRESSION
P_s
V_s
η_0=Y_s=1.6
1.0
0.5
0.2
0.1
0.05
S=0.20
0.10
0.05
0.025

FIG. 2-6

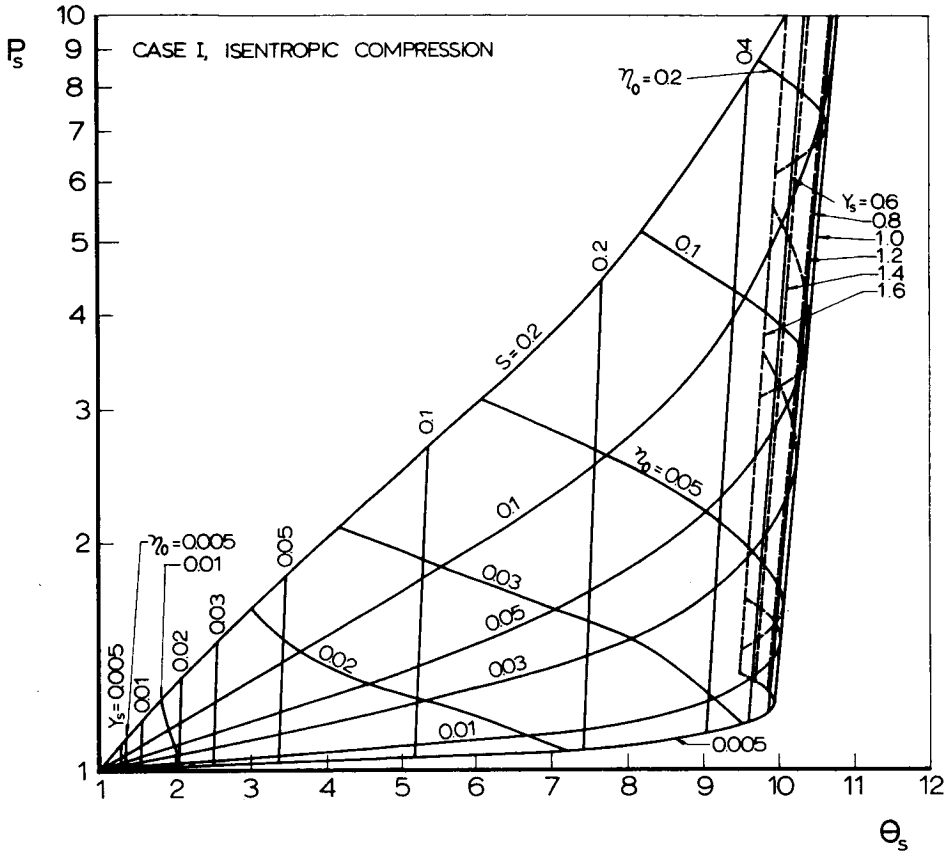
CASE I, ISENTROPIC COMPRESSION
P_s
θ_s
η_0=0.2
0.4
Y_s=0.6
0.8
1.0
1.2
1.4
1.6
S=0.2
0.1
0.2
η_0=0.005
0.1
0.005
η_0=0.0005
0.01
0.003
0.02
0.003
0.001
Y_s=0.0005
0.005
0.002
0.01
0.0005

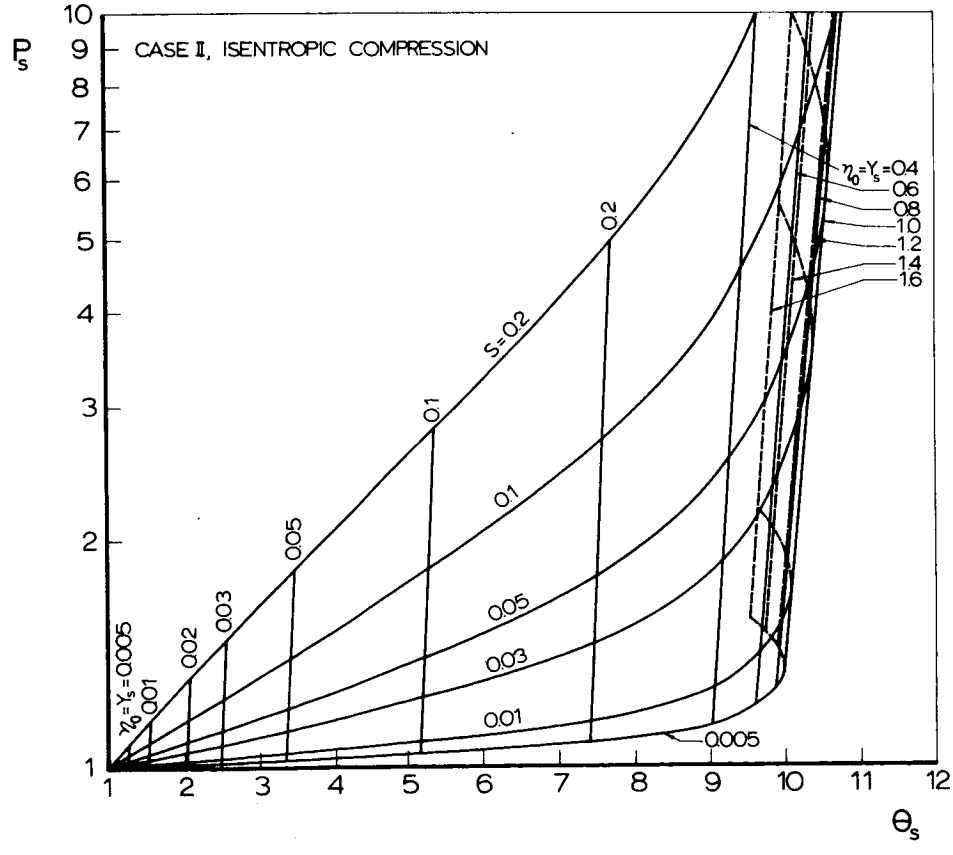
CASE II, ISENTROPIC COMPRESSION
P_s
θ_s
η_0=Y_s=0.4
0.6
0.8
1.0
1.2
1.4
1.6
S=0.2
0.2
0.1
0.1
0.005
0.05
0.003
η_0=Y_s=0.0005
0.001
0.002
0.003
0.01
0.005
0.0005

FIG. 2-7

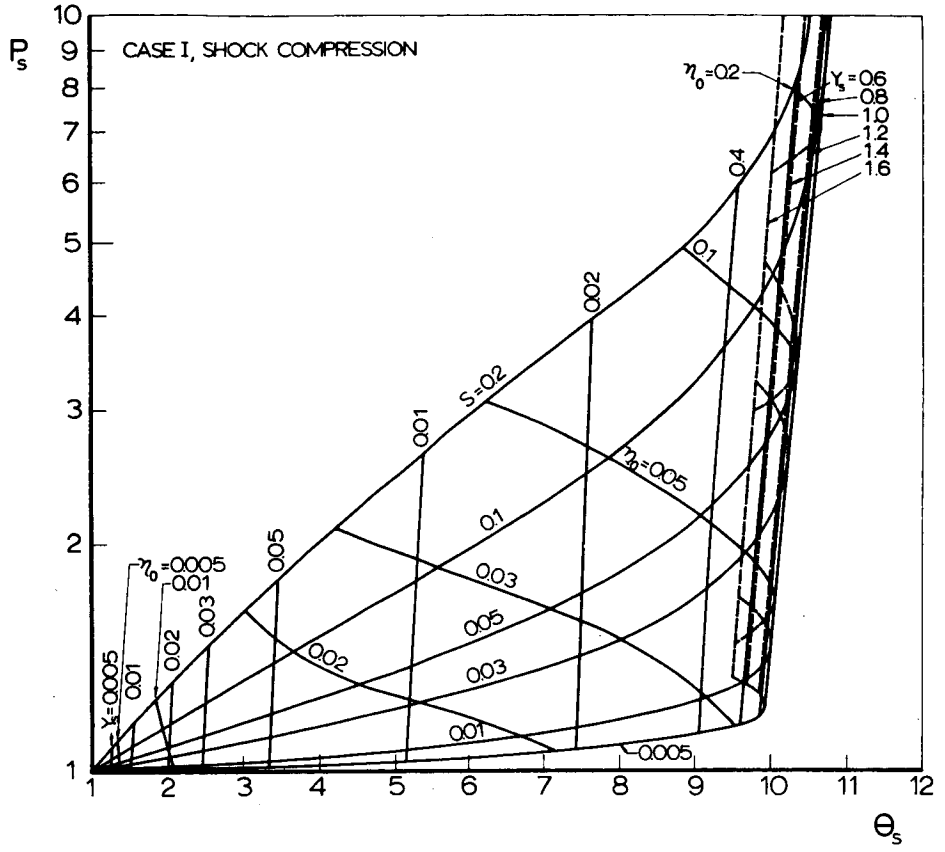
CASE I, SHOCK COMPRESSION
P_s
θ_s
η_0=0.2
γ_s=0.6
0.8
1.0
1.2
1.4
1.6
0.4
0.1
0.02
0.01
S=0.2
η_0=0.005
0.1
0.03
0.005
0.003
0.001
0.005
η_0=0.0005
0.001
0.005
0.003
0.02
0.01
γ_s=0.0005

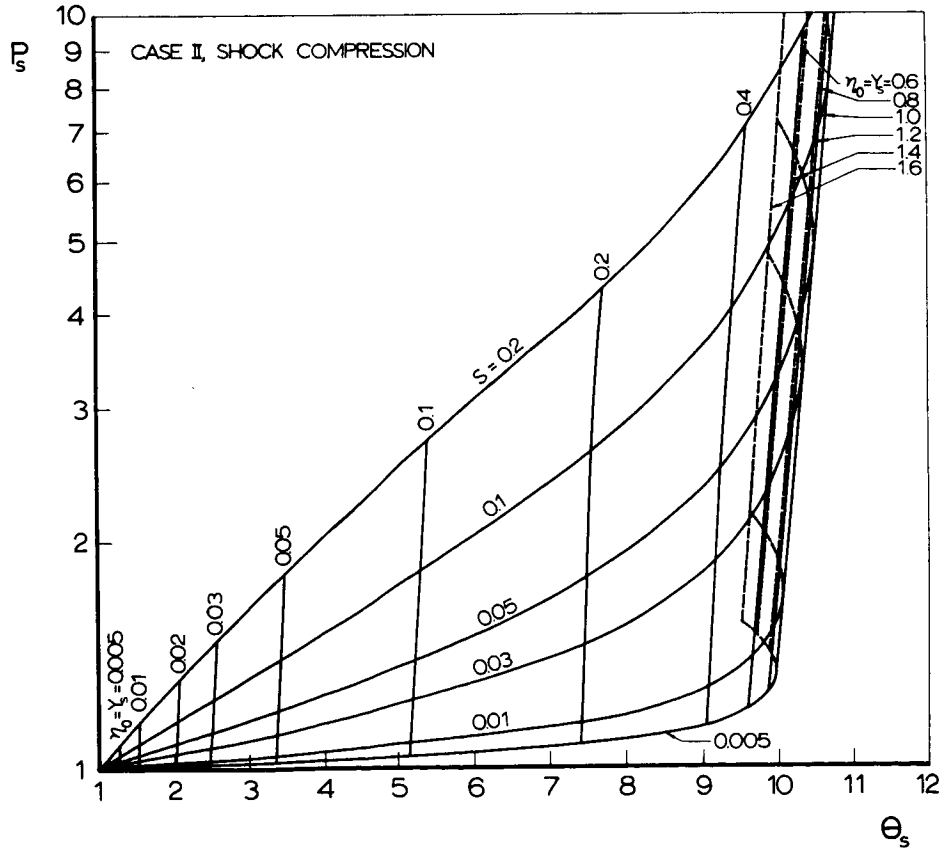
CASE II, SHOCK COMPRESSION
P_s
θ_s
η_0=γ_s=0.6
0.8
1.0
1.2
1.4
1.6
0.4
0.2
0.1
S=0.2
0.1
0.05
0.03
0.001
0.005
0.005
0.003
0.002
0.01
η_0=γ_s=0.005

FIG. 2-8

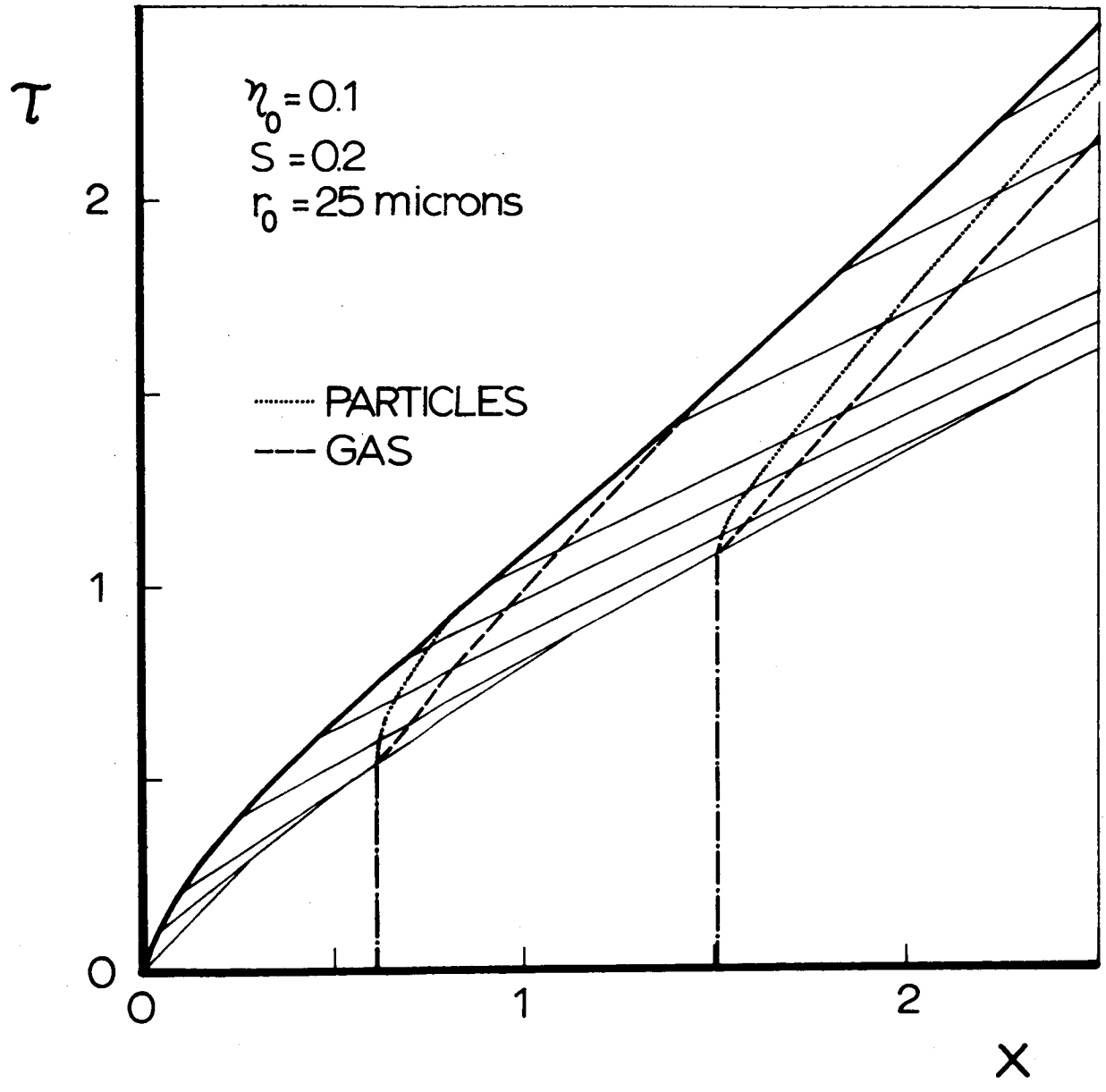

FIG. 3-1

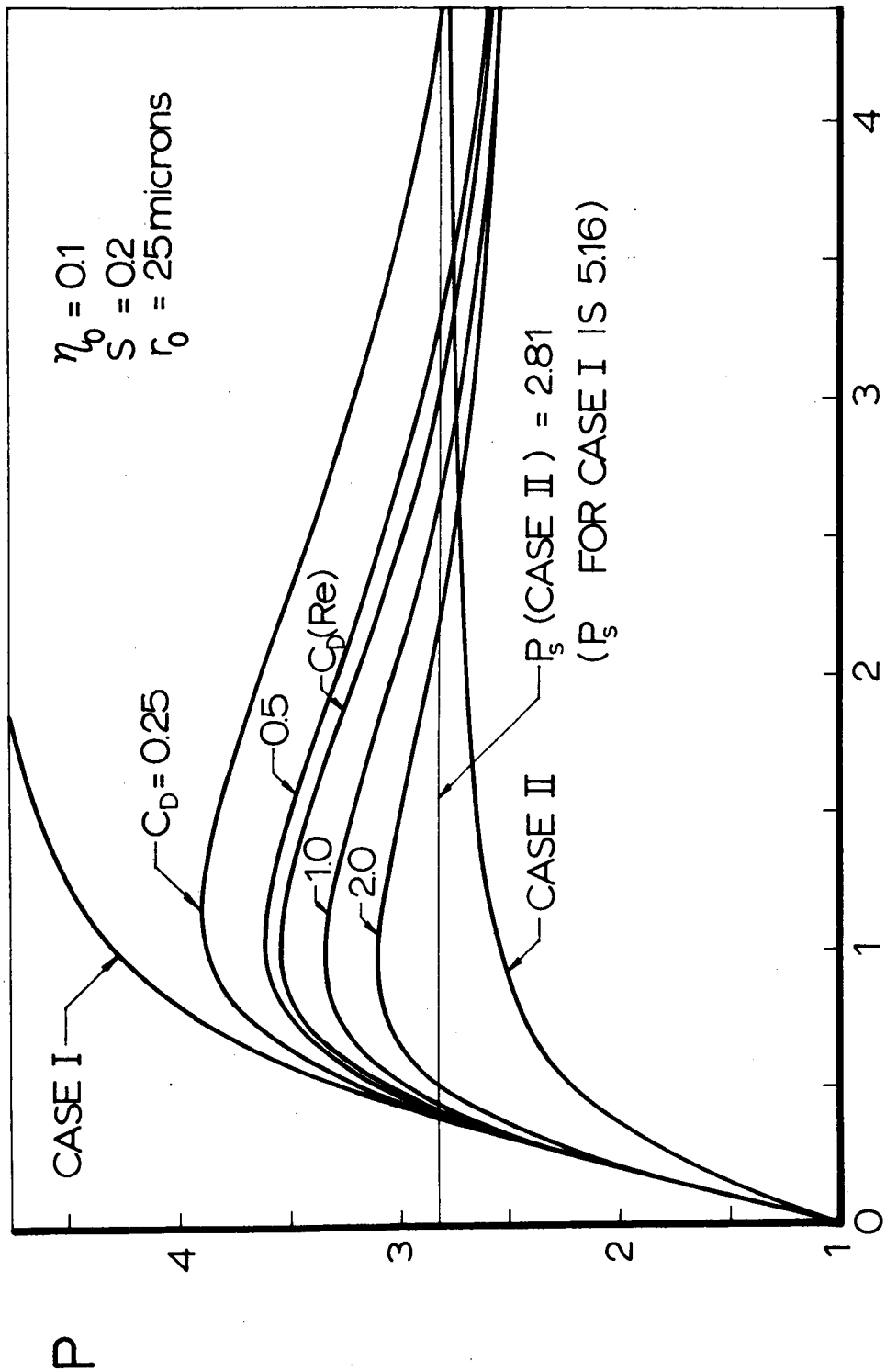
P
τ
CASE I
$C_D = 0.25$
0.5
$C_D(Re)$
1.0
2.0
CASE II
P_s (CASE II) = 2.81
(P_s FOR CASE I IS 5.16)
$\eta_0 = 0.1$
$S = 0.2$
$r_0 = 25$ microns
0
1
2
3
4
1
2
3
4

FIG. 3-2

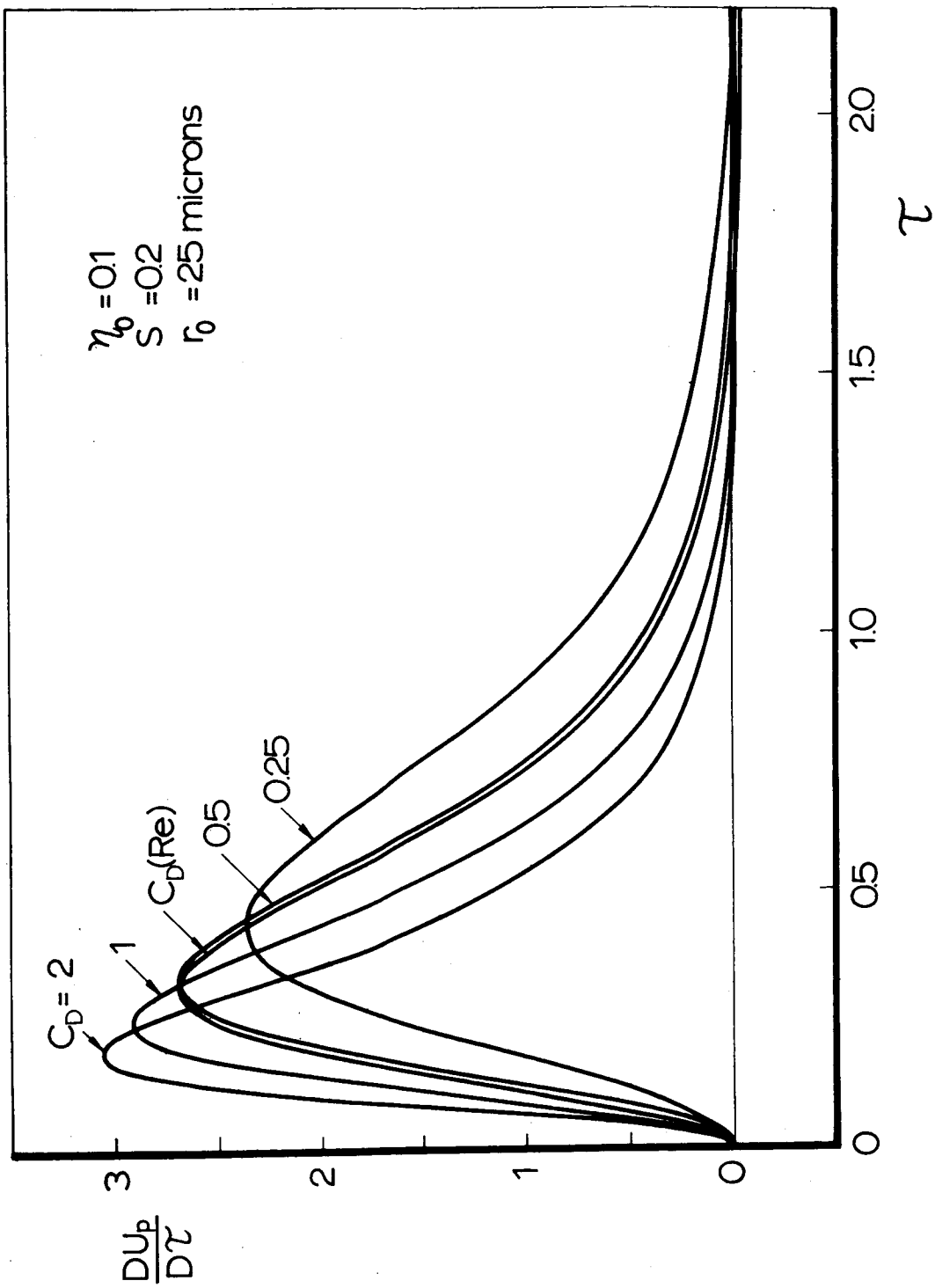
$\eta_0 = 0.1$
$S = 0.2$
$r_0 = 25$ microns
$C_D = 2$
1
$C_D(Re)$
0.5
0.25
$\frac{DU_p}{D\tau}$
3
2
1
0
0
0.5
1.0
1.5
2.0
τ

FIG. 3-3

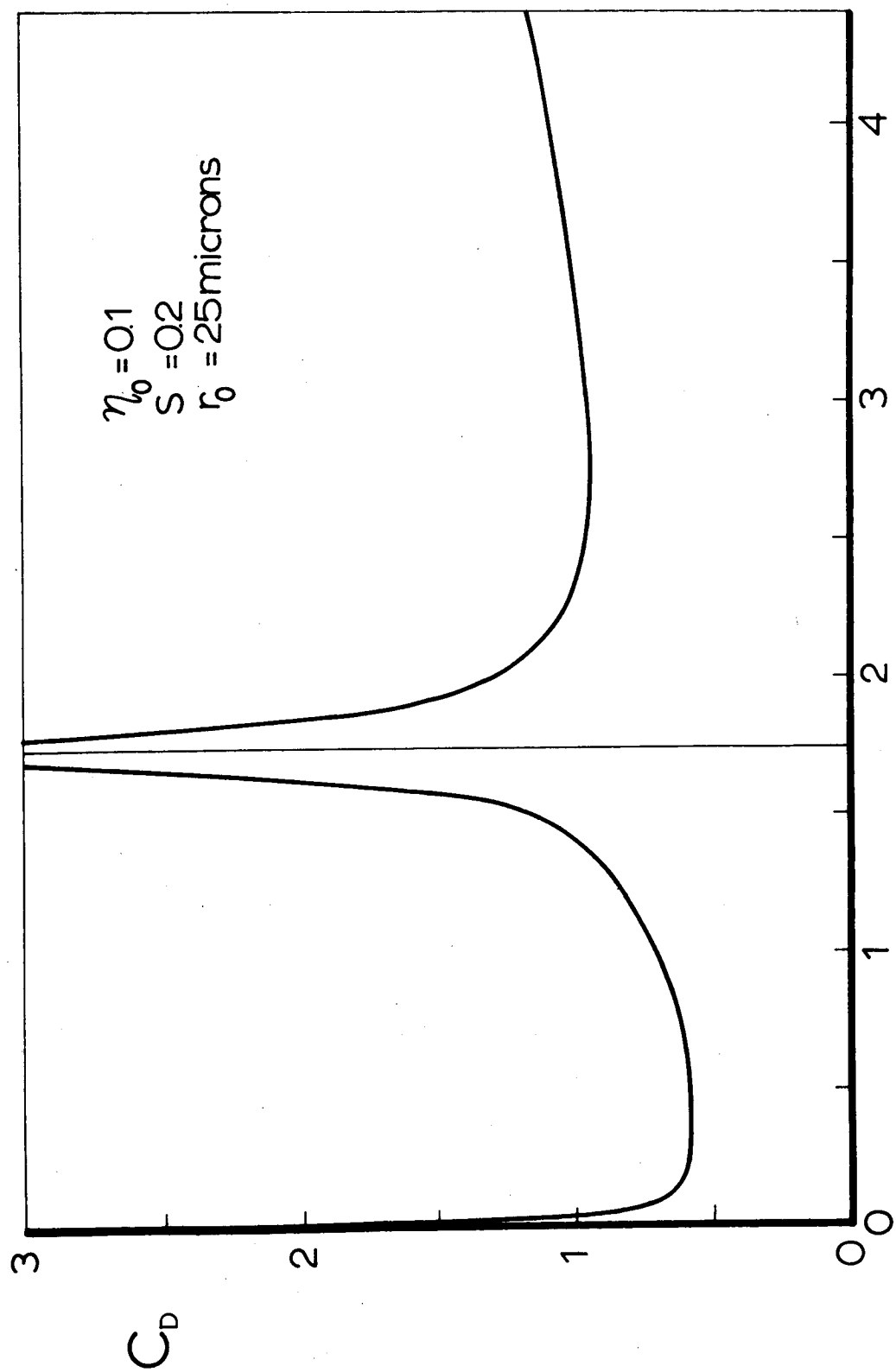

FIG. 3-4

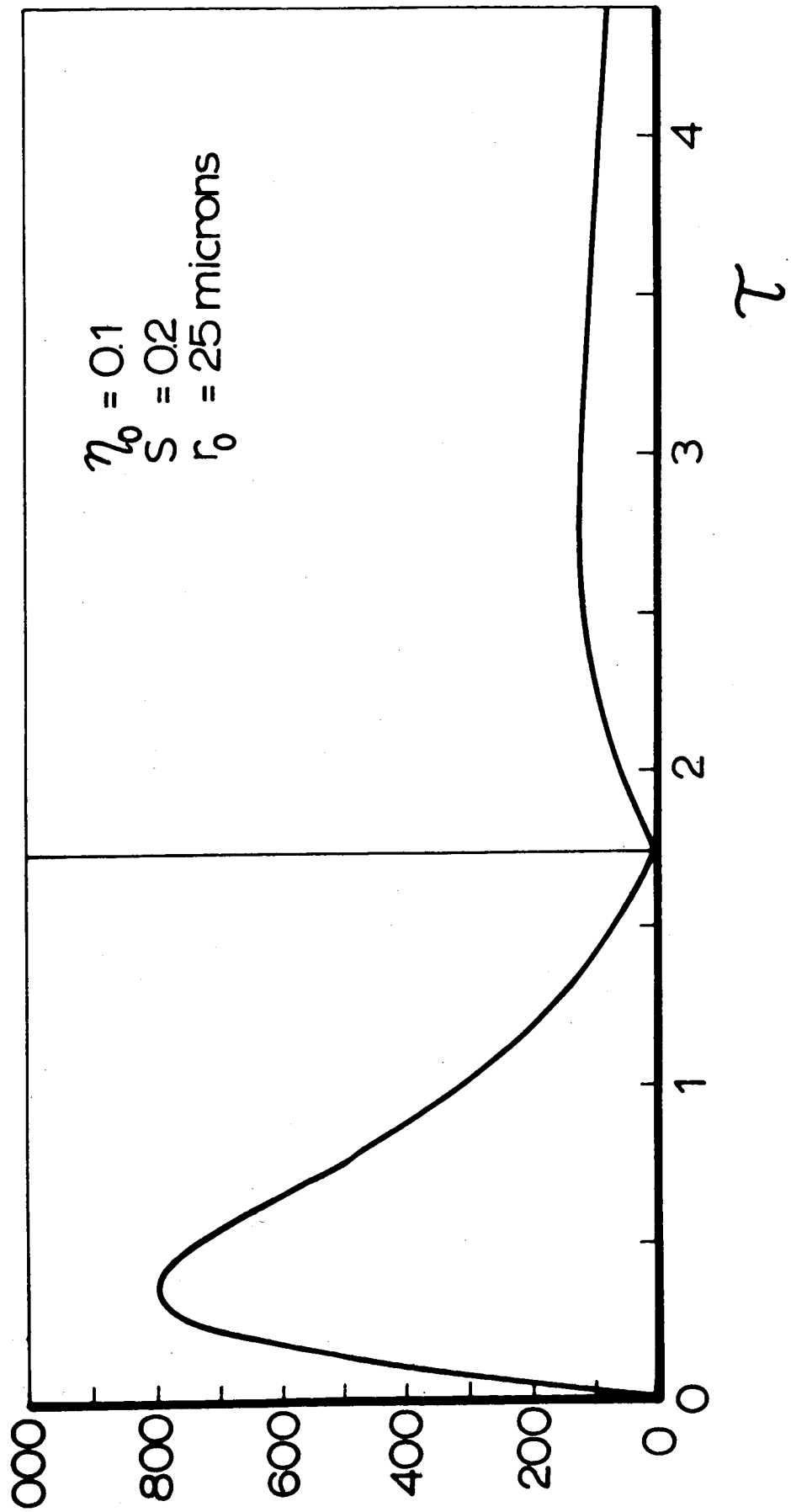

FIG. 3-5

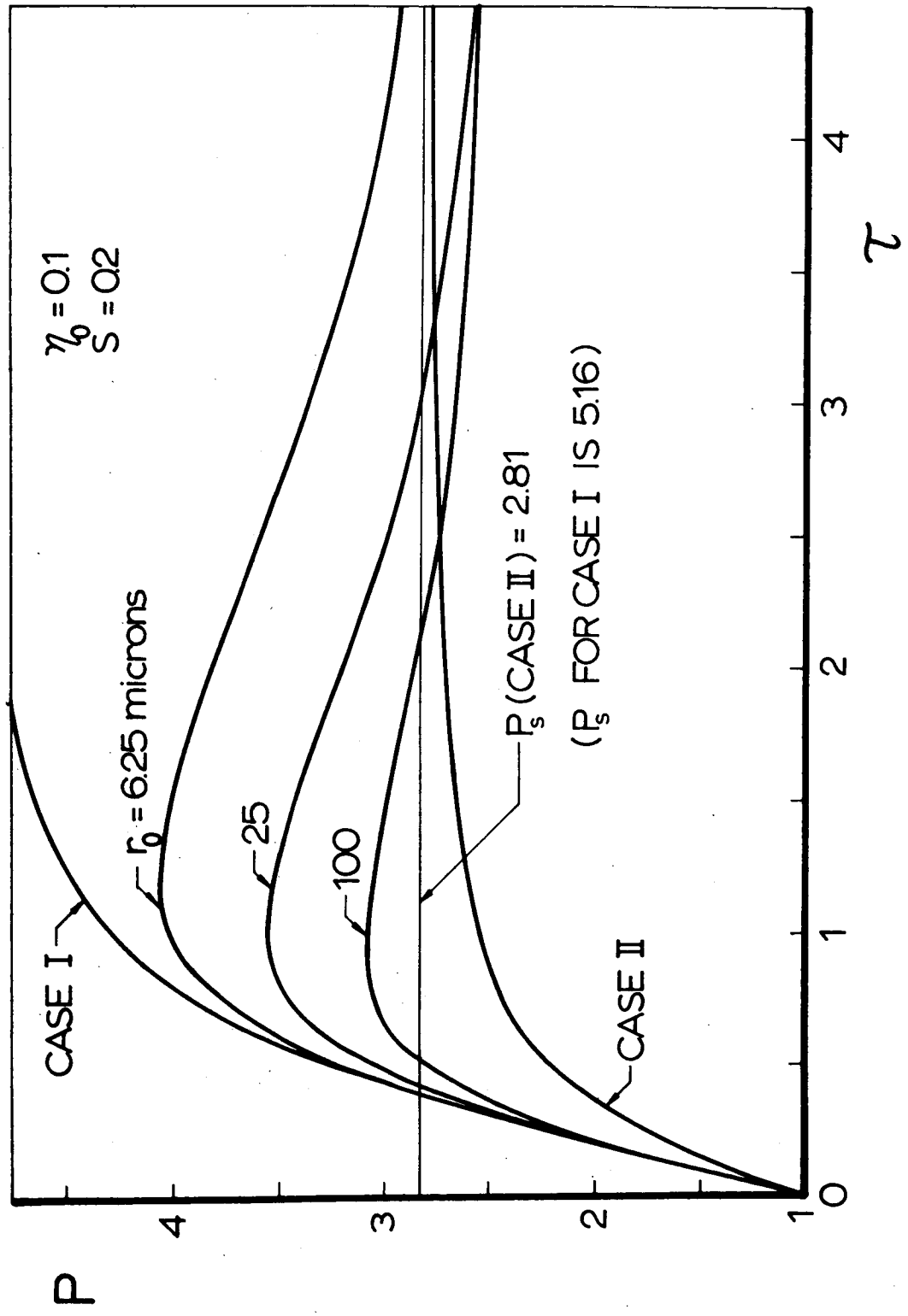
P
τ
0
1
2
3
4
CASE I
r_0 = 6.25 microns
25
100
P_s (CASE II) = 2.81
(P_s FOR CASE I IS 5.16)
CASE II
η_0 = 0.1
S = 0.2

FIG. 3-6

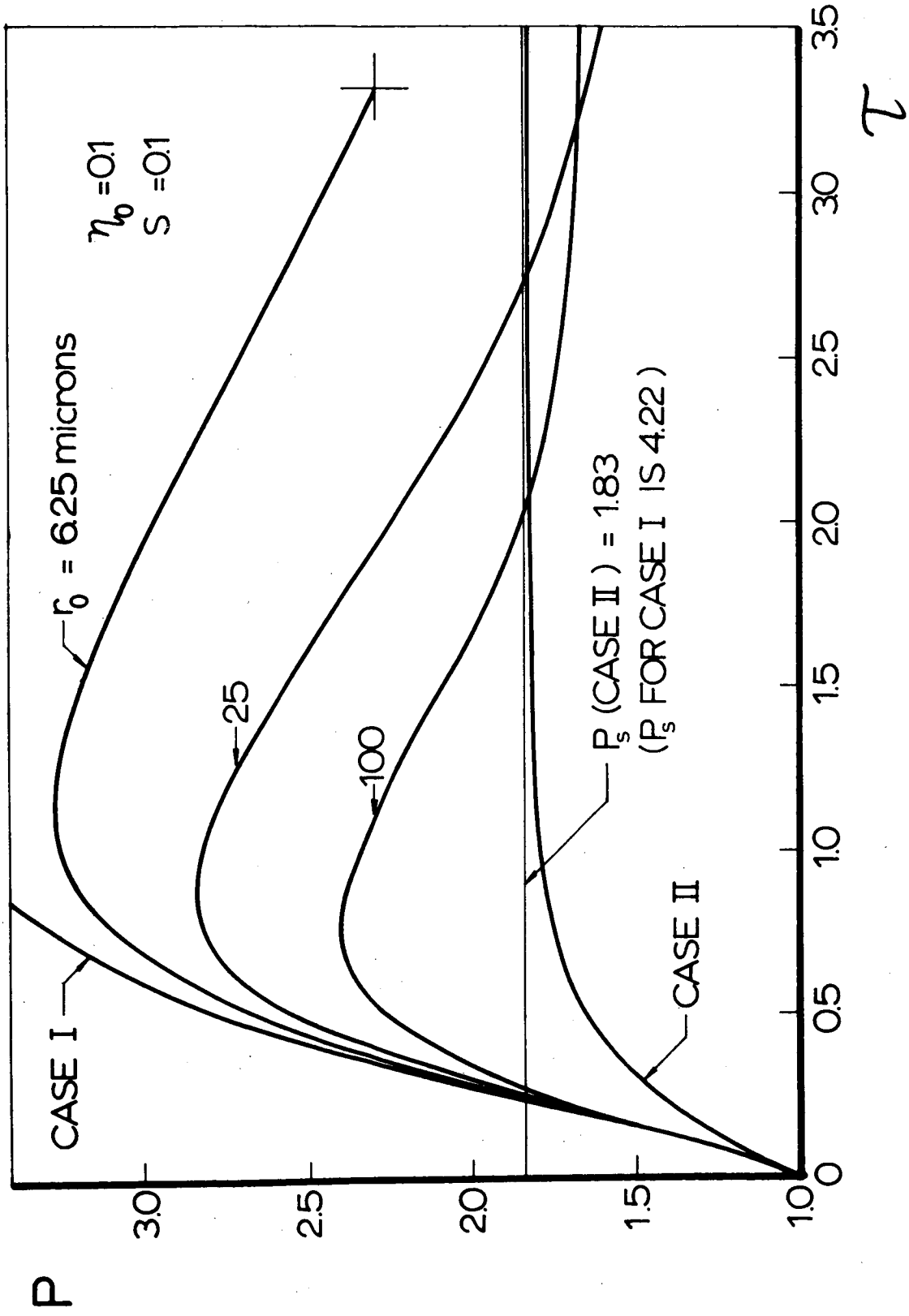
P
3.0
2.5
2.0
1.5
1.0
0
0.5
1.0
1.5
2.0
2.5
30
3.5
τ
CASE I
r_0 = 625 microns
25
100
η_0 =0.1
S =0.1
P_s (CASE II) = 1.83
(P_s FOR CASE I IS 4.22)
CASE II

FIG. 3-7

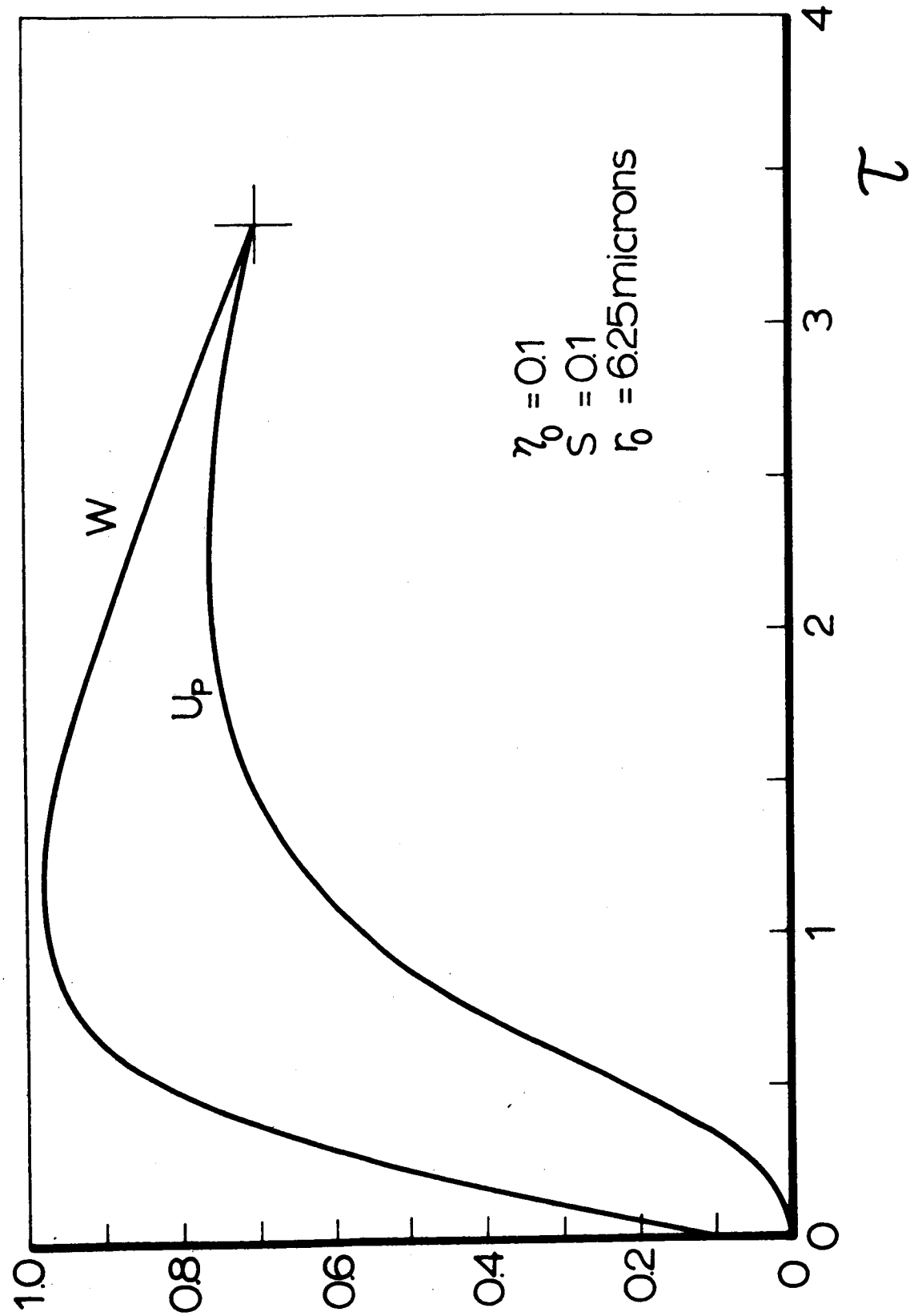

FIG. 3-8

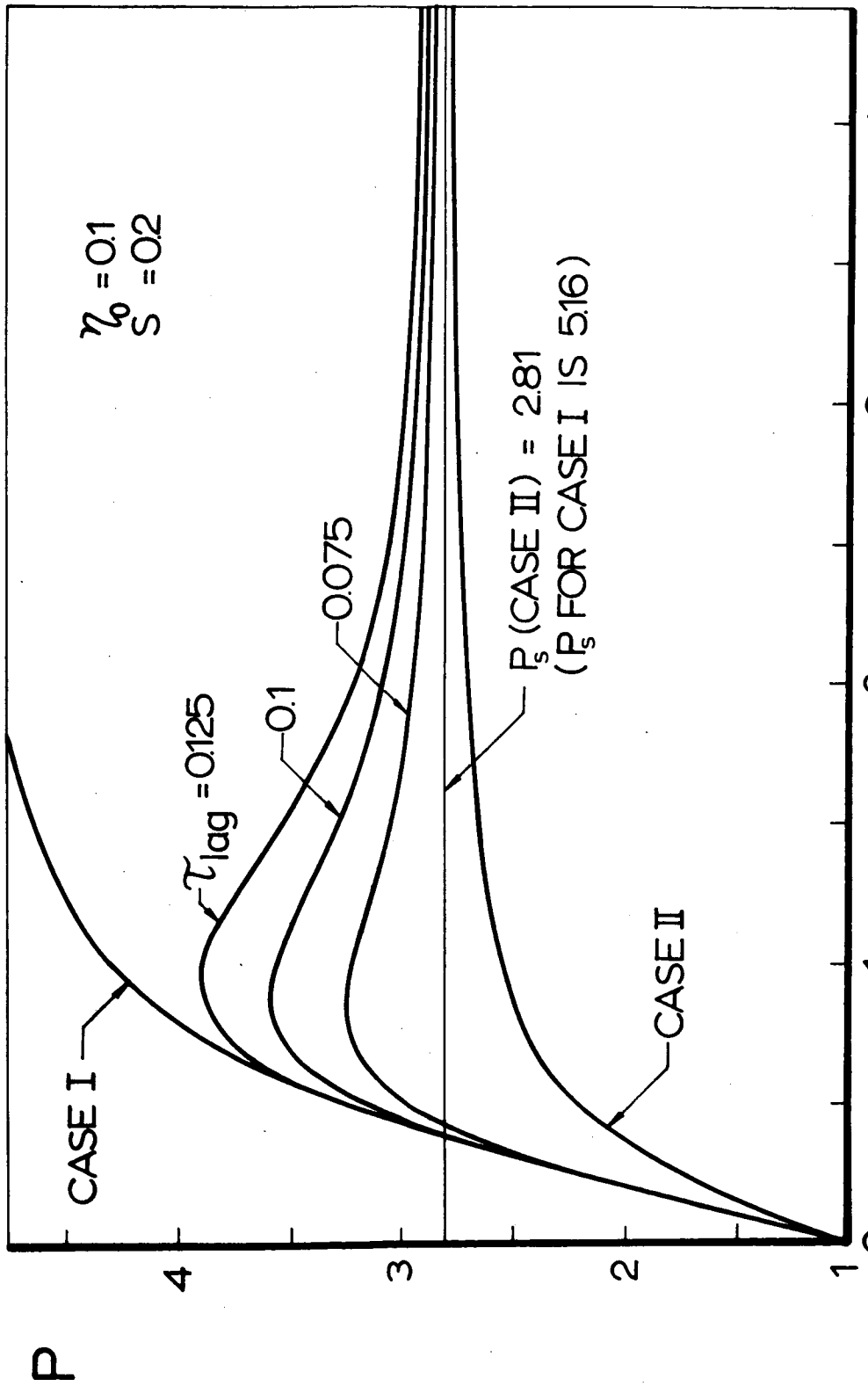
P
τ
η_o = 0.1
S = 0.2
CASE I
τ_{lag} = 0.125
0.1
0.075
P_s (CASE II) = 2.81
(P_s FOR CASE I IS 5.16)
CASE II
0
1
2
3
4

FIG. 3-9

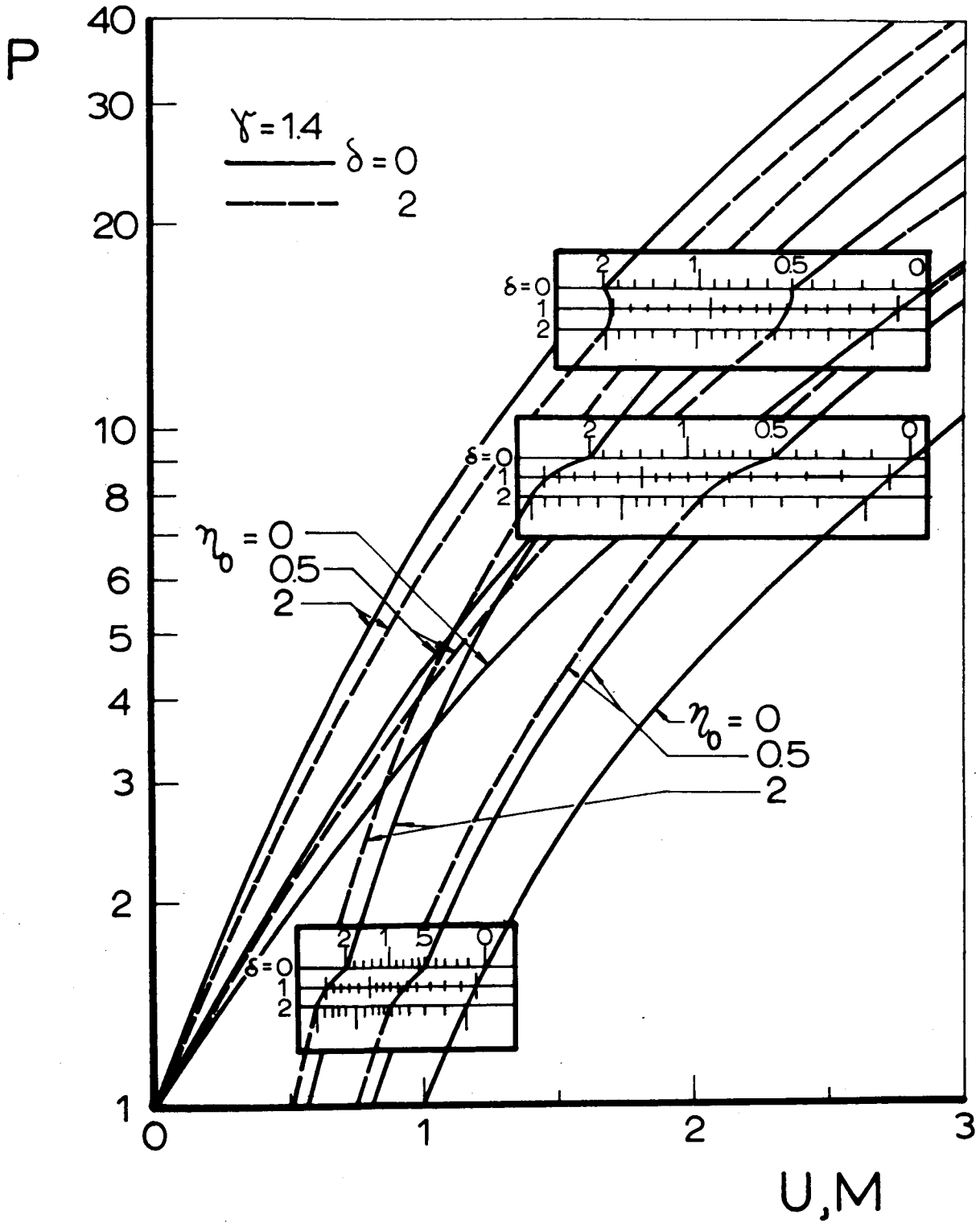
P
40
30
20
10
8
6
5
4
3
2
1
0
1
2
3
U,M
γ = 1.4
δ = 0
2
η0 = 0
0.5
2
η0 = 0
0.5
2
δ = 0
1
2
2
1
0.5
0
δ = 0
1
2
2
1
0.5
0
δ = 0
1
2
2
1
5
0

FIG. 4-1

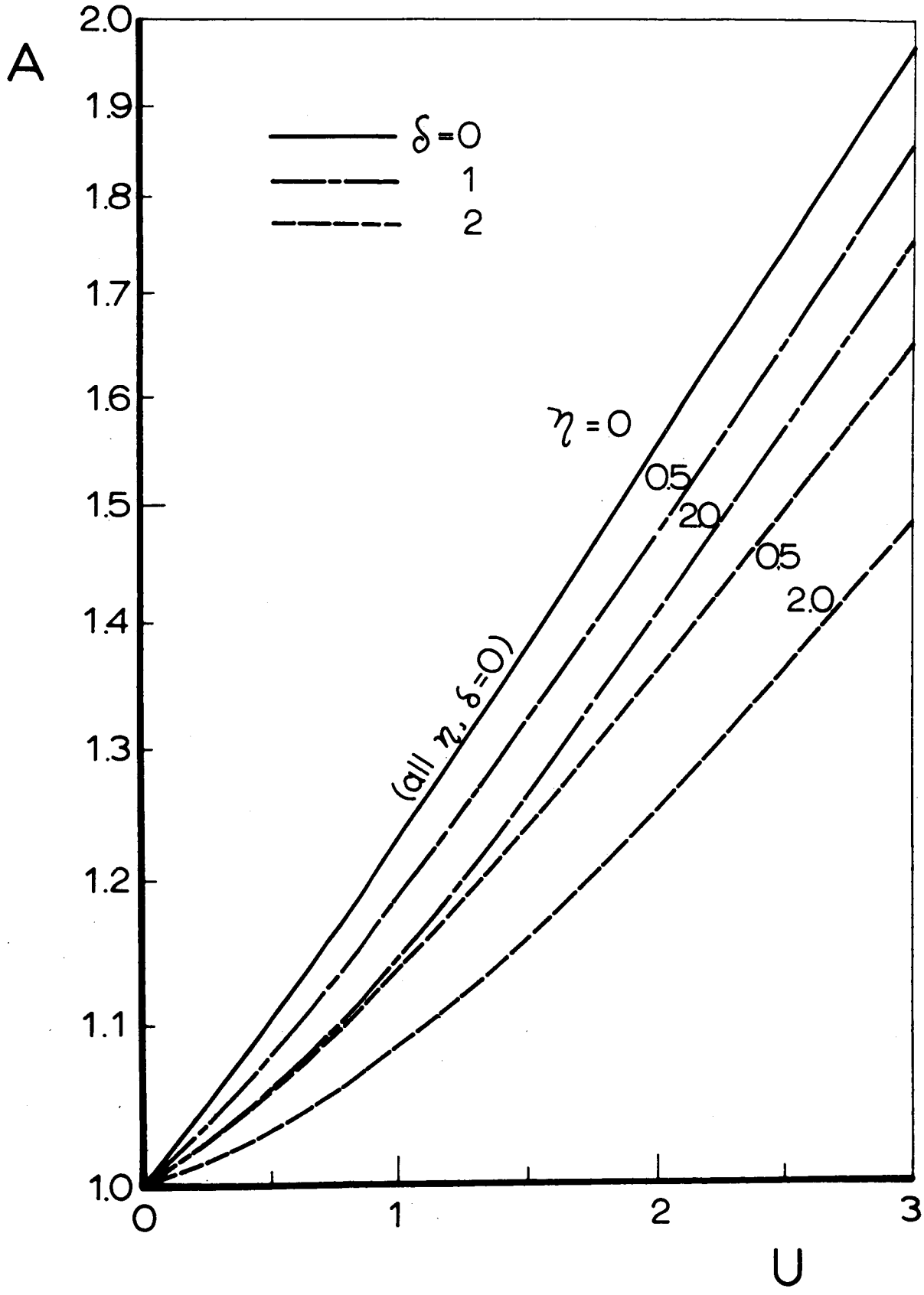

FIG. 4-2

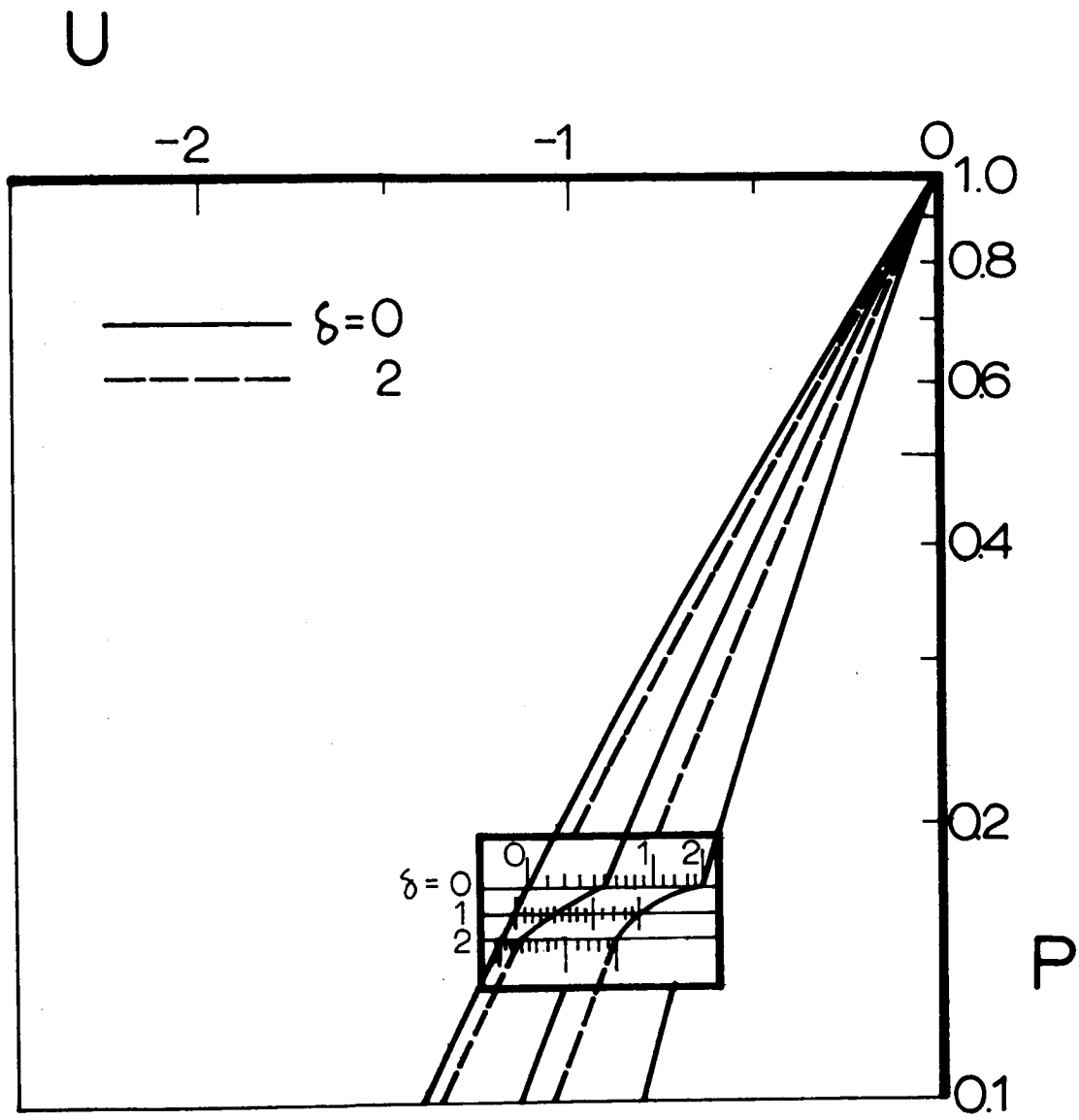

FIG. 4-3

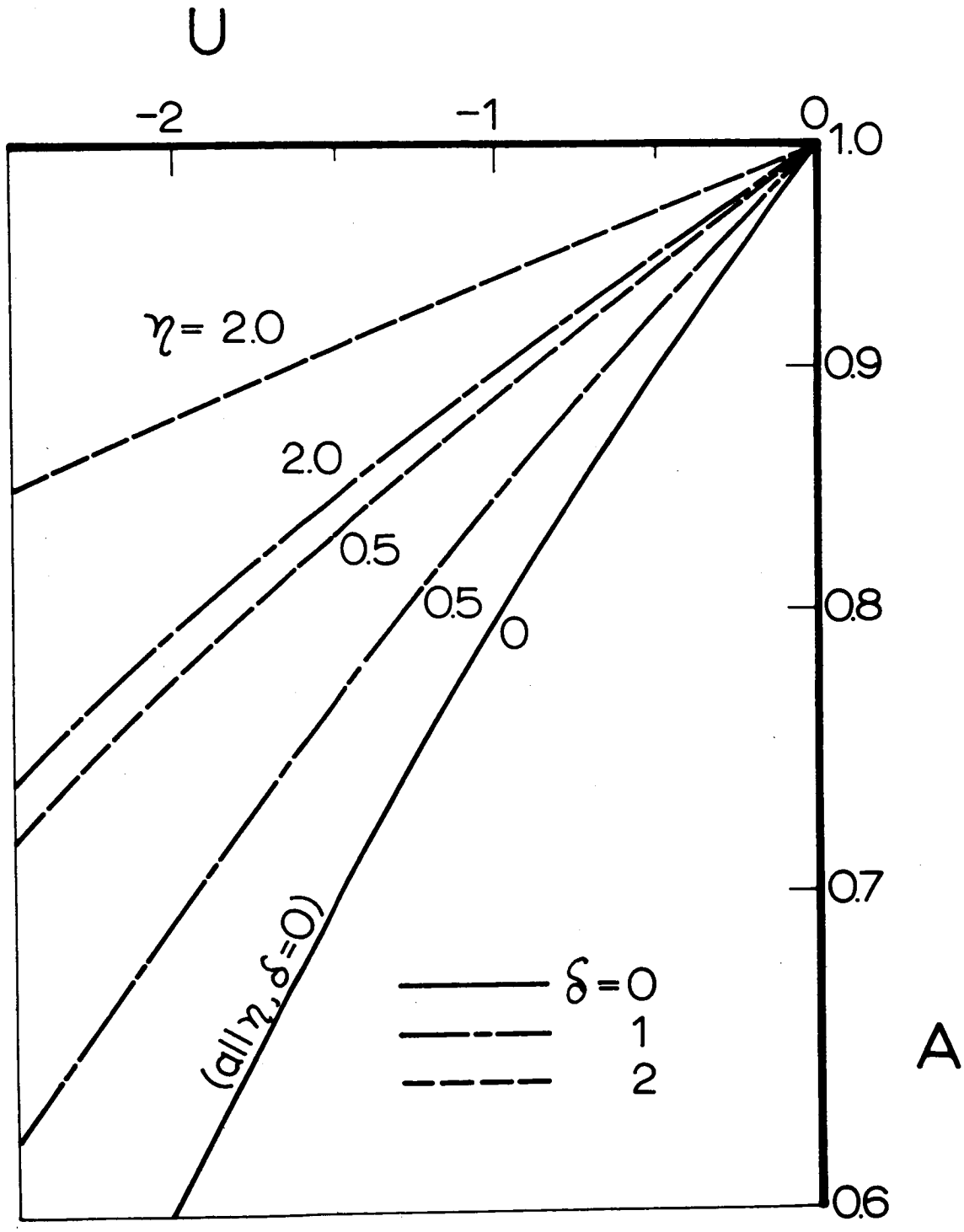

FIG. 4-4

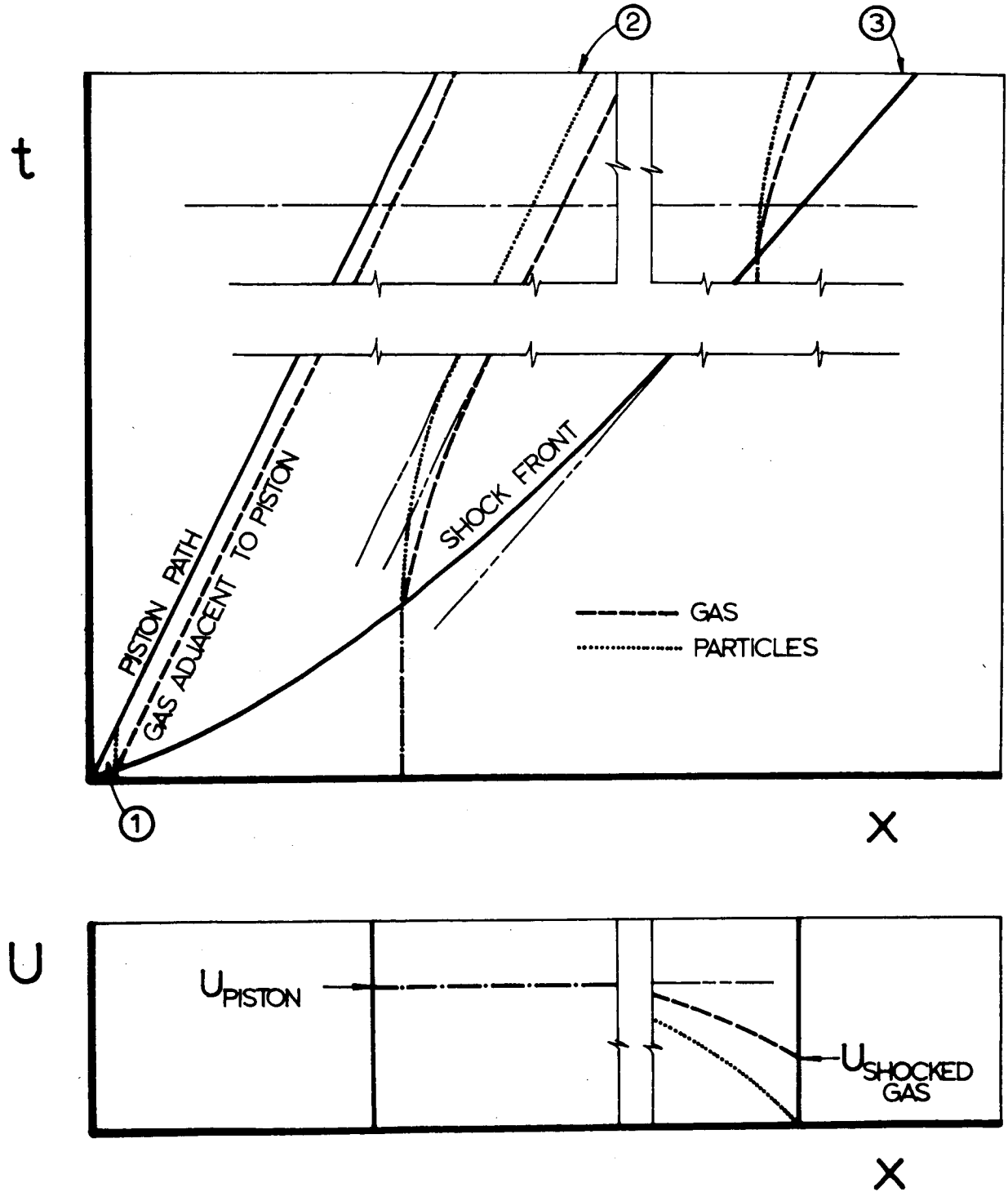
t
2
3
PISTON PATH
GAS ADJACENT TO PISTON
SHOCK FRONT
GAS
PARTICLES
1
X
U
U PISTON
U SHOCKED GAS
X

FIG. 4-5

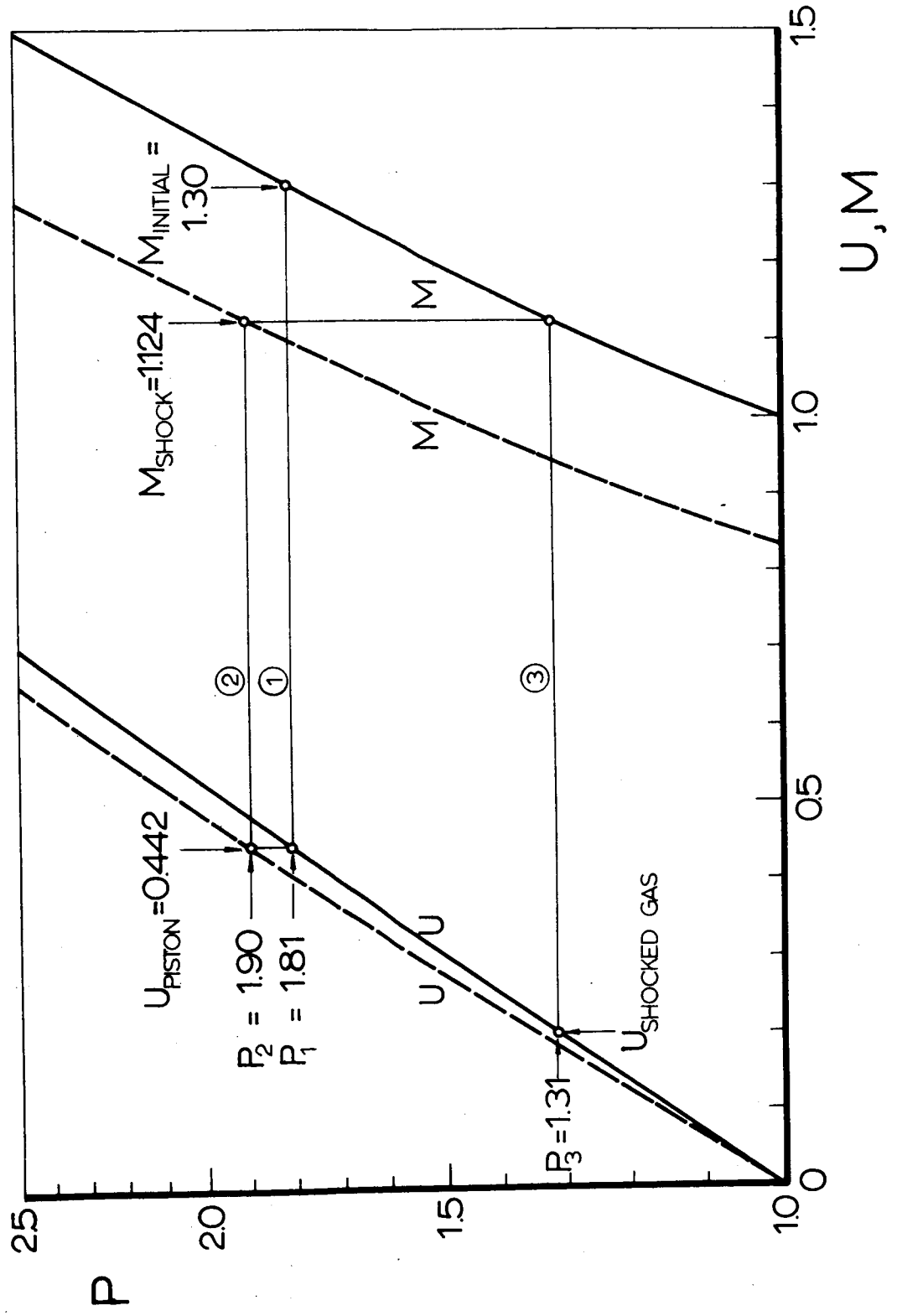
P
2.5
2.0
1.5
1.0
0
0.5
1.0
1.5
U, M
$M_{INITIAL}$ = 1.30
M_{SHOCK}=1.124
M
M
U
U
U_{PISTON}=0.442
P_2 = 1.90
P_1 = 1.81
P_3=1.31
$U_{SHOCKED\ GAS}$
①
②
③

FIG. 4-6